

The authors would like to thank the Anonymous Referee 1 for his/her valuable comments and suggestions to strengthen the analysis presented in our manuscript. The comments and suggestions have been taken into account in the revised manuscript, as follows (original referee's comments in bold):

**This study used a biogeochemical model to examine effects of climate forcing biases in global climate reanalysis on carbon cycle predictions across a permafrost peatland thaw gradient. The main findings show that all peatland sites studied (bog, fen, palsa) remain carbon sinks, but that the bog and fen have a net positive radiative forcing because of high methane emissions. The study finds that climate responses can have major implications for carbon cycle dynamics in these systems. It is well written. Just a few comments below to help clarify some of the site descriptions, etc.**

The authors thank the reviewer for the valuable comments. We have carefully revised our manuscript based on the suggestions provided by the reviewer to clarify some of the original descriptions.

**Specific comments:**

**Line 63-69: what about the mass-balance studies from Alaska that suggest that a significant portion of the permafrost peat is lost upon thaw (O'Donnell et al., 2014 Ecosystems, Jones et al., 2016 Global Change Biology).**

O'Donnell et al. (2012) and Jones et al. (2017) have been included in our revised manuscript (Lines 66-71) to improve our description of permafrost peatland carbon vulnerability under a changing climate.

**Line 135-136: The seasonality of precipitation could be important. Is there information on whether its increased snowfall/depth (which could also warm soil temperatures)?**

The precipitation measured at ANS did not show a significant change in precipitation seasonality throughout the years. Precipitation magnitude and variability during summer are generally greater than during winter (Figure 3b). The analysis presented by Malmer et al. (2005) showed that monthly mean snow depth in 1986-2000 was greater than in 1957-1970, suggesting that it is possible that increased annual precipitation (Figure 2b) can be associated with increased snowfall in winter and spring. Unfortunately, we do not have

continuous snowfall or snow depth measurements to compare with the changes in precipitation.

**Study site description:** has anyone studied the history of permafrost at this site (i.e., when it formed) and whether permafrost aggradation occurred syngenetically with peat accumulation? I would argue that this information is important in carbon dynamics with thaw.

Inception of peat deposition at the Stordalen Mire has been dated at around 6,000 calendar years before present (cal. BP) (Sonesson 1972) in the southern part of the mire and at around 4,700 cal. BP in the northern part (Kokfelt et al., 2010). Kokfelt et al. (2010) suggested that permafrost aggregation initiated during the Little Ice Age (around 120-400 cal. BP) in the Stordalen Mire.

We agree with the reviewer that permafrost history of the study site could be important in carbon dynamics with thaw. However, such information may not affect our analysis because we did not attempt to simulate permafrost aggradation/degradation history in this study. Instead, we simulate the palsa, bog, and fen sites individually and discuss the differences shown in different thaw stages. We did, however, add the peat and permafrost history information to the site description (Lines 146-150).

**Line 161: italicize *Sphagnum***

*Sphagnum* has been italicized as suggested by the reviewer (Line 171).

**Line 173: It is unclear if the measurements described in this paragraph were conducted in this study or if the authors are reporting on measurements made by Bäckstrand et al. Perhaps that can be clarified at the beginning of this paragraph**

The measurements described in this paragraph were made by Bäckstrand et al. (2008b). A proper citation has been added at the beginning of this paragraph (Line 184).

**Line 174-175: “chamber lids were removed in the Fall”: Fall can be lowercase (as can spring, here and elsewhere; you don’t capitalize “summer” later in the text). Can you be more specific about “fall” and “spring”? How closely did the measurements coincide with freeze-up and thaw? Which months? Do you suspect that there are winter emissions? How many chambers/peatland type? Do you have any idea when the fen and bog thawed (i.e., 5 years ago, 500 years ago, 1000 years**

**ago) and when peat started accumulating at these sites? These could have important implications for emissions and the carbon balance of a peatland.**

All seasons have been converted to lowercase in the revised manuscript. We have revised the original sentence with some clarifications for the measurement period (Lines 184-188). We believe that winter emissions could contribute to the annual carbon budget, as suggested by our simulation results, but we don't yet have enough quality-controlled measurements in winter to verify our hypothesis. We don't yet know precisely when the fen and bog formed, but all three of the investigated peatland types were there before 1930's (based on Swedish military photography; information added to the site description (Lines 164-165)). As mentioned above, Kokfelt et al. (2010) suggested that peat inception took place at around 4,700 cal. BP (around 6,000 cal. BP by Sonesson 1972) in the Stordalen Mire and permafrost aggregation initiated during the Little Ice Age.

**Line 365: how much does the water table fluctuate for the bog over the summer?**

The simulated water table fluctuates from -7 cm to -1 cm (below surface) over the summer, as shown in Figure 6.

**Line 408: “the higher CH<sub>4</sub> emissions in the fully thawed fen can be attributed to its faster thaw rate”: Do you mean rate of seasonal thaw or do you mean rate of permafrost thaw? If permafrost thaw, how do you know how quickly it thawed?**

We meant the rate of seasonal thaw, not the rate of permafrost thaw. We simulated the seasonal thaw dynamics under three different permafrost thaw stages, and compared the seasonal thaw and carbon cycling across the permafrost thaw gradient. The original sentence has been revised as suggested by the reviewer (Line 421).

**Section 4.1, ~line 415: in addition to ALD, do you know if there is a talik in any of these peatland types in the winter? Also, I don't understand why the “fully thawed fen” or the bog have an ALD, if they're thawed. Perhaps a conceptual diagram would help readers envision the differences in permafrost regime of these different peatland types, or at least clarification about what is meant by ALD in the “fully thawed fen” and bog. An additional table might be useful that includes information about total peat depth, active layer depths, average water table depths, surface vegetation communities, and perhaps some information on the number of chambers per site (and was just one feature per peatland type studied or did you study multiple?)?**

The water table depth and ALD were only measured in the growing season, and we do

not know if there is a talik in our study sites during winter. The confusing description (fully thawed fen) has been replaced with “fen” in the revised manuscript. The original terminology was chosen to match previous studies conducted at the same sites that qualitatively describes the permafrost thaw gradient across palsa, bog, and fen.

As suggested by the reviewer, an additional conceptual diagram (Figure 1) has been included in the revised manuscript to provide a qualitative summary of the three peatland types investigated in this study.

**Line 481-482: Is the model dynamic? Is vegetation allowed to change as conditions change (wetter, drier), or did the model not run long enough for species changes to occur?**

Vegetation is allowed to change with changing environmental conditions, and we noticed species changes among different model forcing climate conditions (results not shown). The *ecosys* model prognoses vegetation dynamics with internal resource allocation and remobilization, competition for light and nutrients, and different plant functional traits. Shifts in plant functional types were modeled through processes of plant functional type competition for light, water, and nutrients (nitrogen, and phosphorus) within each canopy and rooted soil layer. A qualitative summary of the *ecosys* model has been included in the supplemental material of this manuscript.

## Reference

Kokfelt, U., Reuss, N., Struyf, E., Sonesson, M., Rundgren, M., Skog, G., Rosen, P., and Hammarlund, D.: Wetland development, permafrost history and nutrient cycling inferred from late Holocene peat and lake sediment records in subarctic Sweden, *J. Paleolimn.*, 44, 327–342, doi:10.1007/s10933-010-9406-8, 2010.

Malmer, N., Johansson, T., Olsrud, M. and Christensen, T. R.: Vegetation, climatic changes and net carbon sequestration in a North-Scandinavian subarctic mire over 30 years, *Global Change Biology*, 11(11), 1895–1909, doi:10.1111/j.1365-2486.2005.01042.x, 2005.

Oksanen PO (2006) Holocene development of the vaisjeaëggi palsa mire, finnish lapland. *Boreas* 35:81–95.

Sonesson M (1972) Cryptogams. In: International biological programme—Swedish tundra biome project. Technical report No. 9, April 1972. Swedish Natural Science

Research Council Ecological Research Committee

Zuidhoff F, Kolstrup E (2000) Changes in palsa distribution in relation to climate change in Laivadalen, northern Sweden, especially 1960–1997. *Permafrost Periglac* 11:55–59

The authors would like to thank the Anonymous Referee 2 for his/her valuable comments and suggestions to strengthen the analysis presented in our manuscript. The comments and suggestions have been taken into account in the revised manuscript, as follows (original referee's comments in bold):

**General comments: This study applied the ecosys model to predict soil thaw dynamics, NEE, and CH<sub>4</sub> fluxes across a permafrost thaw gradient encompassing palsa, bog, and fen at a subarctic peatland. The authors also investigated impacts of potential climate bias on the simulated active layer depth (ALD), NEE, and CH<sub>4</sub> fluxes. My major concern is that this manuscript is lacking of clearness for methods and explanation/discussion for some results. While the authors cited a lot of ecosys related references, it is not clear how this model simulate ALD, water table, NEE, and CH<sub>4</sub> fluxes (i.e. lacking of the model structure/principle/processes related to these variables) and how the authors set different parameters for palsa, bog, and fen to simulate these variables for different land types (i.e. lacking of description for setting of some parameters; please check specific points). I therefore suggest adding these contents. In addition, I noticed some indigestible results, but did not find explanations/discussions related to these results (check specific comments). I suggest adding explanations/discussions for these results.**

The authors thank the reviewer for the valuable comments, which we believe have improved the manuscript substantially. We have included a qualitative summary of the *ecosys* model to improve our model structure description. We have included the list of parameters we used for our simulation to improve our parameter description. We have included the necessary explanations and discussions requested by the reviewer to improve the clarity of our manuscript.

**Specific comments:**

**Line 151: ALD should be defined at the first place of 'active layer depth'.**

We have now defined ALD as 'active layer depth' at the first place of its presence (Line 108).

**Line 151: For clarity, I suggest changing '35 cm' to '35 cm below the peat surface'.**

We have applied the wording suggested by the reviewer to improve clarity (Line 160).

**Lines 240 to 241: Did you mean that you used the climate data from 1901 to 2010 for model initialization? If so, which year's results were used for analysis?**

The climate data from 1901 to 2001 were used for model initialization (i.e., spinup) and those from 2002 to 2010 were used for analysis. We have clarified this approach in the revised Methods section (Lines 254-255)

**Line 268: How about the values for bog?**

Rydén et al. (1980) did not specify the differences between bog and fen, so we applied the same soil bulk density values for the upper part of the bog and fen sites. We have included a table (Supplemental Material Table 1) to specify some of the key model parameters used in our simulation.

**Lines 264 to 274: How about the vegetation parameters for these three land types?**

Vegetation parameters at the three peatland types were assigned by the observed plant species (section 2.1; Figure 1). The palsa, bog, and fen sites were composed by 4 (shrubs, mosses, sedges, and lichens), 2 (mosses and sedges), and 1 (sedges) plant functional types, respectively.

**Lines 296 to 298: In this sentence, did you want to say inter-annual variability of GSWP3 temperature is smaller in summer. If so, I suggest adding information of the inter-annual variability, in addition to information of underestimation.**

The inter-annual variability information has been added to this sentence (Lines 314-316).

**Lines 336 to 337: This is not accurate; I noticed some points of net CO<sub>2</sub> emission during summer from the figure 4.**

The sentence has been revised to account for the CO<sub>2</sub> emission events during summer (Line 355).

**Line 345: What is the meaning of 'different subsites' in this and other places? Different chambers for a peatland type?**

'Different subsites' was used to indicate different automated chambers for a given peatland type. We have annotated the definition of subsites to improve the clarity of our manuscript (Lines 189 and 363).

**Lines 351 to 356: I noticed consistent over-predictions of net CO<sub>2</sub> uptake for bog. Could you please provide some explanations?**

The authors agree with the reviewer that the simulated net CO<sub>2</sub> uptake, indicated as

negative NEE, were sometimes greater than the measured values during summer. The over-predictions of net CO<sub>2</sub> uptake for the bog could be due to overestimated plant biomass or overestimated CO<sub>2</sub> uptake rate per biomass. However, we currently don't have data to examine the actual cause of overestimated net CO<sub>2</sub> uptake for the bog since the CO<sub>2</sub> flux derived from automated chambers only represents the aggregated results of all controlling factors. An additional dataset of plant biomass (for mosses and sedges at individual automated chamber locations) is needed to examine the cause of overestimated net CO<sub>2</sub> uptake for bog.

**Lines 372 to 375: It is not clear for me how the authors simulated different water table for different land types without considering lateral water transport. Was the simulated different WT driven by different ET among the types since they had the same rainfall? In addition, why this is 'a particular issue' for bog considering that fen receives a large amount of water from a lack (Line 153)?**

The WTD in *ecosys* is calculated at the end of each time step as the depth to the top of the saturated zone below which air-filled porosity is zero. Changes in the simulated water table (WT) were driven by dynamical interactions among precipitation, ET, vertical water transport, and lateral water transport. An external WT was prescribed in our simulations, and that WT interacts with our one-dimensional gridcell. However, the one-dimensional simulation cannot account for lateral water transport among landscape features within a system. For example, no additional water could be transported from the neighboring grids to lift local WT, and no excessive water could be transported to the neighboring grids to deepen local WT. We believe that such processes could be important in determining local WT, but those effects could not be represented in our one-dimensional column simulation. Although both bog and fen WTs were affected by the limitations of our one-dimensional column simulation, it could be more of a concern for bog because the measured WT variability is stronger in bog than those in fen.

**Line 390: The 'weaker CH<sub>4</sub> emission variability measured across subsites' is confusing.**

This sentence was meant to indicate that the variability of CH<sub>4</sub> emissions measured across subsites (automated chambers) within a given peatland type was weaker than CO<sub>2</sub> variability, so increased temporal resolution (helpful for reducing variability across subsites) did not improve our evaluation of CH<sub>4</sub> emissions. This sentence has been revised to improve its clarity (Lines 408-410).

**Line 399: I cannot catch this sentence. The model can produce hourly/daily results,**



**so it is easily to calculate seasonal cumulative NEE directly using the simulations. Why you calculate it based on the seasonality identified in another paper?**

We calculated seasonal cumulative NEE directly using our simulation results, but with the green and snow seasonality instead of the quarterly seasonality. We chose to apply the green and snow seasonality identified in Bäckstrand et al. (2010) to help facilitate the inter-comparison of carbon budgets estimated in the Stordalen Mire, and to better capture the actual seasonality recorded at the study site.

**Lines 427 to 429: Could you please explain why the simulated ALDs at palsa and fen under cold and wet conditions are shallower than that under cold conditions? This seems not consistent with the comparisons between wet and control.**

The simulated ALDs in BIASED-WET were deeper than those in CTRL because the increased snowpack depth keeps the soil warmer with lower soil ice content during winter. A similar snowpack warming mechanism was found in the comparisons between BIASED-COLD and BIASED-COLD&BIASED-WET (i.e., soil ice content was lower with the additional snowpack from the wet biases); however, summertime soil heating in some of the simulation years was not strong enough to thaw the soil ice between 20-40 cm completely with the cold biases. The presence of ice in the middle of the soil column in the BIASED-COLD&BIASED-WET run thus reduces the simulated ALD in some of the simulation years and results in shallower mean ALD as compared to the BIASED-COLD run. These descriptions have now been added to the revised manuscript (Lines 449-452).

**Lines 451 to 452: Why the fen showed weak CO<sub>2</sub> emissions under cold and wet conditions and net CO<sub>2</sub> uptake under cold conditions, due to reduced NPP and/or increased soil respiration under wetter conditions? I cannot understand the large impacts of wet on CO<sub>2</sub> emissions at fen given that WT is close to or above ground surface for this site (Figure 5).**

The vegetation structure and function simulated in *ecosys* dynamically respond to changes in environmental conditions. The amount of sedges simulated in the fen becomes lower under colder/wetter environment (BIASED-COLD/ BIASED-WET vs. CTRL), which slightly weakens the simulated CO<sub>2</sub> uptake strength (Figure 9a). When cold and wet biases are coupled together, simulated CO<sub>2</sub> uptake in the fen was substantially reduced in the BIASED-COLD&BIASED-WET run due to increased oxygen stress. Therefore, the simulated GPP/NPP is significantly reduced in the BIASED-COLD&BIASED-WET run, which shifts the fen toward a weak source of CO<sub>2</sub> emissions

(Figure 9a). These descriptions have now been added to the revised manuscript (Lines 474-475).

**Lines 483 to 487: Could you explain the simulated negative impacts of wet on CH<sub>4</sub> emissions at bog and fen; in particular for the cold and wet scenario, why the CH<sub>4</sub> emissions was simulated close to zero?**

As described above, the presence of wet biases (BIASED-COLD and BIASED-COLD&BIASED-WET) reduces oxygen exchange, which reduces heterotrophic respiration, microbial biomass, and the amount of CH<sub>4</sub> production. The reduction of sedges under wetter environment (BIASED-COLD and BIASED-COLD&BIASED-WET) weakens aerenchyma transport, which also limits CH<sub>4</sub> emissions. When cold and wet biases are coupled together, both of these effects (reduced CH<sub>4</sub> production and weaker aerenchyma transport) strongly inhibit CH<sub>4</sub> emissions and greatly reduce the simulated CH<sub>4</sub> exchanges in the bog and fen sites. These descriptions have now been added to the revised manuscript (Lines 509-512).

1 Large carbon cycle sensitivities to climate across a permafrost thaw gradient in subarctic  
2 Sweden

3  
4 Kuang-Yu Chang\*,  
5 Climate and Ecosystem Sciences Division, Lawrence Berkeley National Laboratory,  
6 Berkeley, California, USA

7 William J. Riley,  
8 Climate and Ecosystem Sciences Division, Lawrence Berkeley National Laboratory,  
9 Berkeley, California, USA

10 Patrick M. Crill,  
11 Department of Geological Sciences, Stockholm University, Stockholm, Sweden

12 Robert F. Grant,  
13 Department of Renewable Resources, University of Alberta, Edmonton, Alberta, Canada

14 Virginia I. Rich,  
15 Department of Microbiology, The Ohio State University, Columbus, Ohio, USA

16 and,  
17 Scott R. Saleska,  
18 Department of Ecology and Evolutionary Biology, University of Arizona, Tucson,  
19 Arizona, USA

20  
21  
22 \*Corresponding author: Kuang-Yu Chang, ckychang@lbl.gov

23 Climate and Ecosystem Sciences Division, Lawrence Berkeley National Laboratory  
24 Berkeley, California, USA

25 Phone: (510) 495-8141

## Abstract

Permafrost peatlands store large amounts of carbon potentially vulnerable to decomposition. However, the fate of that carbon in a changing climate remains uncertain in models due to complex interactions among hydrological, biogeochemical, microbial, and plant processes. In this study, we estimated effects of climate forcing biases present in global climate reanalysis products on carbon cycle predictions at a thawing permafrost peatland in subarctic Sweden. The analysis was conducted with a comprehensive biogeochemical model (*ecosys*) across a permafrost thaw gradient encompassing intact permafrost palsa with an ice core and a shallow active layer, partly thawed bog with a deeper active layer and a variable water table, and fen with a water table close to the surface, each with distinct vegetation and microbiota. Using *in situ* observations to correct local cold and wet biases found in the Global Soil Wetness Project Phase 3 (GSWP3) climate reanalysis forcing, we demonstrate good model performance by comparing predicted and observed carbon dioxide (CO<sub>2</sub>) and methane (CH<sub>4</sub>) exchanges, thaw depth, and water table depth. The simulations driven by the bias-corrected climate suggest that the three peatland types currently accumulate carbon from the atmosphere, although the bog and fen sites can have annual positive radiative forcing impacts due to their higher CH<sub>4</sub> emissions. Our simulations indicate that projected precipitation increases could accelerate CH<sub>4</sub> emissions from the palsa area, even without further degradation of palsa permafrost. The GSWP3 cold and wet biases for this site significantly alter simulation results and lead to erroneous active layer depth (ALD) and carbon budget estimates. Biases in simulated CO<sub>2</sub> and CH<sub>4</sub> exchanges from biased climate forcing are as large as those among the thaw stages themselves at a landscape-scale across the

49 examined permafrost thaw gradient. Future studies should thus not only focus on changes  
50 in carbon budget associated with morphological changes in thawing permafrost, but also  
51 recognize the effects of climate forcing uncertainty on carbon cycling.

## 1. Introduction

Confidence in future climate projections depends on the accuracy of terrestrial carbon budget estimates, which are presently very uncertain (Friedlingstein et al., 2014; Arneeth et al., 2017). In addition to the complexity in physical process representations, a major source of this uncertainty comes from challenges in quantifying climate responses induced by biogeochemical feedbacks. Increases in atmospheric carbon dioxide (CO<sub>2</sub>) concentrations can directly stimulate carbon sequestration from plant photosynthesis (Cox et al., 2000; Friedlingstein et al., 2006) and indirectly stimulate carbon emissions (e.g., from soil warming and resulting increased respiration), although the predicted magnitudes of these exchanges strongly depend on model process representations (Zaehle et al., 2010; Grant, 2013, 2014; Ghimire et al., 2016; Chang et al., 2018).

The undecomposed carbon stored in permafrost is of critical importance for biogeochemical feedbacks to climate because it is about twice as much as currently is in the atmosphere (Hugelius et al., 2014) and is vulnerable to release to the atmosphere as permafrost thaws (Schuur et al., 2015). O'Donnell et al. (2012) suggested that permafrost thaw would result in a net loss of soil organic carbon from the entire peat column because accumulation rates at the surface were insufficient to balance deep soil organic carbon losses upon thaw. Jones et al. (2017) indicated that the loss of sporadic and discontinuous permafrost by 2100 could result in a release of up to 24 Pg of soil carbon from permafrost peatlands to the atmosphere. Lundin et al. (2016) reported that it is plausible (71% probability) for the high latitude terrestrial landscapes to serve as a net carbon source to the atmosphere, although its peatland components would remain atmospheric carbon sinks.

In addition to the overall carbon balance of the changing Arctic, the type of carbon gaseous emission is important to climate feedbacks. High latitudes are predicted to get wetter (IPCC, 2014), and saturated anaerobic conditions facilitate methane (CH<sub>4</sub>) production, which is a much more efficient greenhouse gas than CO<sub>2</sub> in terms of global warming potential. Even habitats that can be net carbon sinks can produce positive radiative forcing impacts on climate due to CH<sub>4</sub> release, as Bäckstrand et al. (2010) showed for a subarctic peatland. Under projected warming and wetting trends in the Arctic (Collins et al., 2013; Bintanja and Andry, 2017), carbon cycle feedbacks over the permafrost region could become stronger as increased precipitation enhances surface permafrost thaw and strengthens CH<sub>4</sub> emissions by expansion of anaerobic volume (Christensen et al., 2004; Wickland et al., 2006).

The Stordalen Mire in northern Sweden (68.20°N, 19.05°E) is in the discontinuous permafrost zone, encompassing a mosaic of thaw stages with associated distinct hydrology and vegetation (Christensen et al. 2004; Malmer et al., 2005), microbiota (Mondav and Woodcroft et al., 2014; Mondav et al., 2017; Woodcroft and Singleton et al., 2018), and organic matter chemistry (Hodgkins et al., 2014). These landscapes have been shifting over the last half-century to a more thawed state, likely due to recent warming (Christensen et al. 2004). Drier hummock sites dominated by shrubs have degraded to wetter sites dominated by graminoids (Malmer et al., 2005; Johansson et al., 2006). The thaw-induced habitat shifts are associated with increases in landscape-scale CH<sub>4</sub> emissions (Christensen et al. 2004; Johansson et al., 2006; Cooper et al., 2017) reflective of the higher CH<sub>4</sub> emissions of the wetter thawed habitats (McCalley et al., 2014). The higher CO<sub>2</sub> uptake in later thaw-stage habitats has not compensated for the



increase in positive radiative forcing from elevated CH<sub>4</sub> emissions (Bäckstrand et al., 2010; Deng et al., 2014).

The impacts of climate sensitivity on the terrestrial carbon cycle have been investigated at the global scale, and the results highlight the need to consider uncertainty in climate datasets when evaluating permafrost region carbon cycle simulations (Ahlström et al., 2017; Guo et al., 2017; Wu et al., 2017). Ahlström et al. (2017) showed that climate forcing biases are responsible for a considerable fraction (~40%) of the uncertainty range in ecosystem carbon predictions from 18 Earth System Models (ESMs) reported by Anav et al. (2013). Guo et al. (2017) concluded that the differences in climate forcing contribute to significant differences in simulated soil temperature, permafrost area, and Active Layer Depth (ALD). Wu et al. (2017) demonstrated that differences among climate forcing datasets contributes more to predictive uncertainty than differences in apparent model sensitivity to climate forcing. However, notably, none of these studies accessed the effects on CH<sub>4</sub> emissions, and their spatial resolution could not represent site-level spatial heterogeneity observed in arctic tundra (Grant et al. 2017a; 2017b).

Here, we use the ecosystem model *ecosys*, which employs a comprehensive set of coupled biogeochemical and hydrological processes, to estimate the effects of climate forcing uncertainty and sensitivity on CO<sub>2</sub> and CH<sub>4</sub> exchanges and ALD simulations. For the Stordalen Mire site, we estimated bias in the Global Soil Wetness Project Phase 3 (GSWP3) climate reanalysis dataset using site-level long-term meteorological measurements and evaluated impacts on simulated soil and plant processes across the permafrost thaw gradient. This approach enables us to assess model sensitivity to

individual climate forcing biases, instead of the aggregated uncertainty range embedded in climate datasets (e.g., variations of climate conditions represented in different climate datasets) presented in previous studies. We address the following questions for our study site at the Stordalen Mire: (1) What are the biases embedded in the GSWP3 climate reanalysis dataset? (2) How do those biases affect model predictions of **ALD**, CO<sub>2</sub> exchanges, and CH<sub>4</sub> exchanges? (3) How does climate sensitivity vary across the stages of permafrost thaw? In addition to improving understanding of permafrost responses to climate, we identify ecosystem carbon prediction uncertainty induced by climate forcing uncertainty in general as the biases found in GSWP3 were consistent with other climate reanalysis datasets during the last decade (section 3).

## **2. Methods and Data**

### **2.1 Study site description**

Our study sites are located at the Stordalen Mire (68.20 °N, 19.03 °E: 351 m above sea level), which is about 10 km southeast of the Abisko Scientific Research Station (ANS) in northern Sweden. Significant changes in climate over this region have been recorded during the last few decades. The annual mean air temperature measured at the ANS has risen by 2.5 °C from 1913 to 2006, where it exceeded the 0 °C threshold (0.6 °C in 2006) for the first time over the past century (Callaghan et al., 2010). The measured annual total precipitation has also increased from 306 mm y<sup>-1</sup> (years 1913 to 2009) to 336 mm y<sup>-1</sup> (years 1980 to 2009) (Olefeldt and Roulet, 2012), along with increased variability in extreme precipitation (Callaghan et al., 2010). The measured annual maximum snow depth has increased from 59 cm (years 1957 to 1971) to 70 cm

(years 1986 to 2000), and the snow cover period with snow depth greater than 20 cm has decreased from 5.8 months (years 1957 to 1971) to 4.9 months (years 1986 to 2000) (Malmer et al., 2005). Inception of peat deposition at the Stordalen Mire has been dated at around 6,000 calendar years before present (cal. BP) (Sonesson 1972) in the southern part of the mire and at around 4,700 cal. BP in the northern part (Kokfelt et al., 2010). Kokfelt et al. (2010) suggested that permafrost aggregation initiated during the Little Ice Age (around 120–400 cal. BP) in the Stordalen Mire.

The Stordalen Mire can be broadly classified into three peatland types: intact permafrost palsa, partly thawed bog, and fen (Hodgkins et al., 2014), hereafter referred to as palsa, bog, and fen (Figure 1). The spatial distribution of these peatland types in 2000 are described in Olefeldt and Roulet (2012). The palsa sites are ombrotrophic and raised 0.5 to 2.0 m above their surroundings, with a relatively thin peat layer (0.4 to 0.7 m, Rydén et al., 1980), thinner active layer depth (less than 0.7 m in late summer), and no measurable water table depth (Bäckstrand et al., 2008a; 2008b; Olefeldt and Roulet, 2012). The bog sites are ombrotrophic and are wetter than the palsa sites, with a thicker peat layer (0.5 to ~1 m, Rydén et al., 1980), deeper ALD (greater than 0.9 m), and water table depth fluctuating from 35 cm below the peat surface to the ground surface (Bäckstrand et al., 2008a; 2008b; Olefeldt and Roulet, 2012). The fen sites are minerotrophic, receiving a large amount of water from a lake to the east of the mire, with water table depths near or above the ground surface (Bäckstrand et al., 2008a; 2008b; Olefeldt and Roulet, 2012). All three of the investigated peatland types were there before 1930's, based on Swedish military photography.

Differences in hydrology and permafrost conditions create high spatial heterogeneity with different soil moisture, pH, and nutrient conditions that support different plant communities (Bäckstrand et al., 2008a; 2008b). The palsa is dominated by dwarf shrubs with some sedges, feather mosses, and lichens (Malmer et al., 2005; Bäckstrand et al., 2008a; 2008b; Olefeldt and Roulet, 2012). The bog is dominated by *Sphagnum* spp. mosses with a moderate abundance of sedges (Malmer et al., 2005; Bäckstrand et al., 2008a; 2008b; Olefeldt and Roulet, 2012). The fen sites we studied are dominated by sedges (Bäckstrand et al., 2008a; 2008b).

## 2.2 Field measurements

Continuous daily meteorological measurements have been recorded at the ANS since 1913, including air temperature, precipitation, wind speed, wind direction, relative humidity, and snow depth. Measurements of solar radiation, longwave radiation, and soil temperature are also available at the ANS since 1982. The soil thaw depth (measured to 90 cm) and water table depth measurements were taken in the three peatland types 3 to 5 times per week from early May to mid-October during 2003 to 2007 (Bäckstrand et al., 2008b).

CO<sub>2</sub> and CH<sub>4</sub> exchanges at the three peatland types were measured with automated chambers during the thawed seasons from 2002 to 2007 (Bäckstrand et al., 2008b). Chamber lids were removed when snow accumulates in winter (around November), and the sampling period for each year ranged from days 87–147 in 2002 (shortest) and days 148–341 in 2005 (longest) (Bäckstrand et al., 2008b; Bäckstrand et al., 2010). Three chambers were in the palsa, three were in the bog, and two were in the

fen (we term each chamber a ‘subsite’ in the following). Each chamber covered an area of 0.14 m<sup>2</sup> with a height of 25–45 cm depending on the vegetation and the depth of insertion and was closed for 5 minutes every 3 hours to measure CO<sub>2</sub> and total hydrocarbon (THC) exchanges. CH<sub>4</sub> exchanges were manually observed approximately 3 times per week, and these measurements were used to quantify the proportion of CH<sub>4</sub> in the measured THC (Bäckstrand et al., 2008a). The CH<sub>4</sub> exchanges were near zero in the palsa sites (Bäckstrand et al., 2008a; Bäckstrand et al., 2008b; Bäckstrand et al., 2010), so they were not used in model evaluation. We used the CO<sub>2</sub> and CH<sub>4</sub> exchanges observed at 3-hourly steps when the R<sup>2</sup> values recorded in the measurements were greater than 0.8 (Tokida et al., 2007), and then calculated the associated daily mean exchanges when there were 8 measurements per day (Table 1). The quality-controlled daily measurements only covered 12.4–33.7% of the daily data points because of the lack of continuous quality-controlled 3-hourly measurements. The data screening was applied to exclude unreliable measurements and avoid biases from inappropriate gap filling, which is necessary for model evaluations. More detailed descriptions of the CO<sub>2</sub> and CH<sub>4</sub> exchanges measurements can be found in Bäckstrand et al. (2008a).

### 2.3 GSWP3

GSWP3 is an ongoing modeling activity that provides global gridded meteorological forcing (0.5° x 0.5° resolution) and investigates changes in energy, water, and carbon cycles throughout the 20<sup>th</sup> and 21<sup>st</sup> centuries. The GSWP3 dataset is based on the 20<sup>th</sup> Century Reanalysis (Compo et al., 2011), using a spectral nudging dynamical downscaling technique described in Yoshimura and Kanamitsu (2008). A more detailed

description of the GSWP can be found in Dirmeyer (2011) and van den Hurk et al. (2016).

In this study, we extracted the meteorological conditions at the Stordalen Mire from 1901 to 2010 from the GSWP3 climate reanalysis dataset. The 3-hourly products of air temperature, precipitation, solar radiation, wind speed, and specific humidity were interpolated to hourly intervals with cubic spline interpolation to serve as the meteorological inputs used in our model.

The GSWP3 dataset was chosen over other existing climate reanalysis datasets for its spatial and temporal resolutions. For example, the Climatic Research Unit (CRU; Harris et al., 2014) dataset provided monthly meteorological forcing at  $0.5^\circ \times 0.5^\circ$  resolution; the National Centers for Environmental Prediction (NCEP; Kalnay et al., 1996; Kanamitsu et al., 2002) dataset provided 6-hourly meteorological forcing at T62 Gaussian grid ( $\sim 1.915^\circ \times 1.895^\circ$  resolution); the CRUNCEP (Viovy, 2018) dataset provided 6-hourly meteorological forcing at  $0.5^\circ \times 0.5^\circ$  resolution; and the European Centre for Medium-Range Weather Forecasts (ECMWF; Berrisford et al., 2011) dataset provided 3-hourly meteorological forcing with 125 km ( $\sim 1.125^\circ$ ) horizontal resolution.

## 2.4 Model description

*Ecosys* is a comprehensive biogeochemistry model that simulates ecosystem responses to diverse environmental conditions with explicit representations of microbial dynamics and soil carbon, nitrogen, and phosphorus biogeochemistry. The aboveground processes are represented in multi-layer plant interacting canopies, and the belowground processes are represented in multiple soil layers with multi-phase subsurface reactive

transport. *Ecosys* operates at variable time steps (down to seconds) determined by convergence criteria, and it can be applied at patch-scale (spatially homogenous one-dimensional) and landscape-scale (spatially variable two- or three-dimensional). Detailed descriptions, including inputs, outputs, governing equations, parameters, and references of the *ecosys* model can be found in Grant (2013). A qualitative summary of the *ecosys* model structure is provided in the supplemental material to this article.

The *ecosys* model has been extensively tested against eddy covariance fluxes and related ecophysiological measurements with a wide range of sites and weather conditions in boreal, temperate, and tropical forests (Grant et al., 2007a; Grant et al., 2007c; Grant et al., 2009a; Grant et al., 2009b; Grant et al., 2009c; Grant et al., 2010), wetlands (Dimitrov et al., 2011; Grant et al., 2012b; Dimitrov et al., 2014; Mezbahuddin et al., 2014), grasslands (Grant and Flanagan, 2007; Grant et al., 2012a), tundra (Grant et al., 2003; Grant et al., 2011b; Grant 2015; Grant et al., 2015), croplands (Grant et al., 2007b; Grant et al., 2011a), and other permafrost-associated habitats (Grant and Roulet, 2002; Grant, 2017a; Grant et al., 2017b). All *ecosys* model structures are unchanged from those described in these earlier studies.

## 2.5 Experimental design

To evaluate the effects of climate on model predictions, we conducted four sets of simulations at each of the three peatland types at the Stordalen Mire from 1901 to 2010. The climate data from 1901 to 2001 were used for model initialization (i.e., spinup) and those from 2002 to 2010 were used for analysis. The 110 year simulations were performed to ensure the simulation was equilibrated with local climate (Grant et al. 2017a).

258           The meteorological conditions for all the simulations were based on the hourly  
259 data extracted from the GSWP3 climate reanalysis dataset (section 2.3). The monthly  
260 mean bias of the GSWP3 for this location was calculated by comparing it to the air  
261 temperature and precipitation measured at the ANS, for years 1913 to 2010 (section 3.1).  
262 The full series of air temperature and precipitation extracted from GSWP3 were then  
263 bias-corrected using the monthly mean bias calculated from 1913 to 2010; we label this  
264 model scenario CTRL. Our bias correction was conceptually similar to the one used in  
265 Ahlström et al. (2017), where the bias-corrected climate forcing fields were the ESM  
266 outputs adjusted by the corresponding bias calculated from observations in a reference  
267 period.

268           The simulation results from CTRL should represent the reliability of applying  
269 *ecosys* at the Stordalen Mire because CTRL is driven by the best local climate  
270 description. We first evaluated predicted thaw depth, water table depth, and CO<sub>2</sub> and CH<sub>4</sub>  
271 exchanges using the CTRL simulation (section 3.2 to 3.4). In the second set of  
272 simulations, BIASED-COLD, the biased GSWP3 air temperature data was used, and we  
273 corrected only the GSWP3 precipitation. Deviations between CTRL and BIASED-COLD  
274 reflect biased air temperature's effects on responses across the thaw gradient. In the third  
275 set of simulations, BIASED-WET, we bias-corrected the air temperature extracted from  
276 GSWP3, which allows us to quantify the effects of biased precipitation. Finally, we used  
277 the meteorological conditions directly extracted from GSWP3 to drive our fourth set of  
278 simulations, BIASED-COLD&BIASED-WET, which reveals the uncertainty range of  
279 subarctic peatland simulation associated with the local biases in GSWP3 climate forcing.



While the three peatland types share the same climate conditions, they differ in soil hydrologic conditions and vegetation characteristics (section 2.1; Figure 1). The bulk density and porosity profiles were set to the values reported in Rydén et al. (1980), who suggested a decreasing trend of bulk density and an increasing trend of porosity from palsa (0.12 Mgm<sup>-3</sup> at surface; 92–93% within the upper 10 cm) to bog and fen (0.06 Mgm<sup>-3</sup> at surface; 96–97% within the upper 10 cm). The peatland soil carbon-to-nitrogen (CN) ratios and pH values were assigned according to Hodgkins et al. (2014), who documented an increasing trend of pH from palsa (4.0), to bog (4.2), to fen (5.7), and a decreasing trend of soil organic matter CN ratio from bog (46±18), to palsa (39±24), to fen (19±0.4). Common values of field capacity (0.4) and wilting point (0.15) were used for the three peatland types (Deng et al., 2014). The soil property parameters used in our simulation for the three peatland types are summarized in Supplemental Material Table1.

### 3 Results and Discussion

#### 3.1 GSWP3 climate comparison to observations

As described in section 2.3, we extracted meteorological conditions at the Stordalen Mire from the GSWP3 climate reanalysis dataset. The closest GSWP3 grid cell was centered at 68.0 °N and 19.0 °E, which covers the Stordalen Mire and the ANS. The annual mean air temperature and precipitation calculated at this GSWP3 grid cell were -3.65 °C and 683.88 mm y<sup>-1</sup>, respectively, for years 1913 to 2010. A cold bias (-3.09 °C) was identified in the GSWP3 annual mean air temperature during the 1913 to 2010 period, although a very high correlation coefficient ( $r = 0.99$ ) was found when compared with the ANS measurements (Figure 2a). Both time series exhibit an overall warming

trend from the early 20<sup>th</sup> century to the present ( $0.01^{\circ}\text{C y}^{-1}$ ), with an even larger warming trend from 1980 to 2010 ( $0.05^{\circ}\text{C y}^{-1}$  [ANS] and  $0.04^{\circ}\text{C y}^{-1}$  [GSWP3]).

Similarly, the GSWP3 annual total precipitation data correlates well with ANS measurements ( $r = 0.80$ ) but has a wet bias of  $380\text{ mm y}^{-1}$  between 1913 and 2010 (Figure 2b). An increasing trend in annual total precipitation was recorded in both time series from the early 20<sup>th</sup> century to present ( $0.47\text{ mm y}^{-2}$  [ANS] and  $1.07\text{ mm y}^{-2}$  [GSWP3]), although a decreasing trend was found from 1980 to 2010 ( $-0.56\text{ mm y}^{-2}$  [ANS] and  $-2.39\text{ mm y}^{-2}$  [GSWP3]).

The seasonal cycle of the GSWP3 monthly mean air temperature also matches that measured at the ANS, with a very high correlation coefficient ( $r = 0.99$ ; Figure 3a). The underestimation bias and inter-annual variability of GSWP3 air temperature are greater in winter (maximum underestimate in December, at  $-4.52^{\circ}\text{C}$  with inter-annual variability of  $3.53^{\circ}\text{C}$ ) and smaller in summer (minimum underestimate in July, at  $-1.52^{\circ}\text{C}$  with inter-annual variability of  $1.65^{\circ}\text{C}$ ), respectively.

The magnitude and inter-annual variability of the GSWP3 monthly mean precipitation are comparable between winter and summer, while the ANS measurements exhibit stronger seasonality with lower magnitudes during winter. Despite the differences found in seasonal patterns, a high correlation coefficient ( $r = 0.64$ ) was found between the monthly mean precipitation extracted from GSWP3 and the ANS measurements. The overestimation of monthly mean precipitation was greatest in December ( $43.25\text{ mm month}^{-1}$ ) and smallest in August ( $18.75\text{ mm month}^{-1}$ ).

These comparisons suggest that GSPW3 air temperature and precipitation data reasonably capture measured seasonal and long-term trends over past decades, but are

biased cold and wet compared to observations, especially during winter. Similar cold and wet biases exist in CRUNCEP and ECMWF climate reanalysis datasets during our 2003 to 2007 study period (Supplemental Material Figure 1). The annual mean air temperature and precipitation at the Stordalen Mire for years 2003 to 2007 were  $-2.49^{\circ}\text{C}$  and  $795.09\text{ mm y}^{-1}$ ;  $-2.46^{\circ}\text{C}$  and  $708.60\text{ mm y}^{-1}$ ; and  $-2.28^{\circ}\text{C}$  and  $765.67\text{ mm y}^{-1}$  in the GSWP3, CRUNCEP, and ECMWF climate reanalysis datasets, respectively.

## 3.2 Model testing

### 3.2.1 Thaw depth

We first evaluated *ecosys* against observations using bias-corrected climate forcing (i.e., the CTRL simulation). Predicted thaw depth agrees well with measurements collected from 2003 to 2007 for all examined peatland types (Figure 4), with a correlation coefficient of 0.95, 0.87, and 0.41 at the palsa, bog, and fen, respectively. Both simulations and observations show that the rate of thaw depth deepening in the summer varies with peatland type (i.e., relatively slow, moderate, and rapid in the palsa, bog, and fen, respectively).

Predicted and observed maximum thaw depth (i.e., ALD) in the intact permafrost palsa was between 45 and 60 cm in September. In the partly thawed bog, the simulated thaw depth is slightly shallower than that observed before August. The simulated bog thaw depth becomes greater than 90 cm by the end of August, which matches the time when measured thaw depth reaches its maximum. The thaw depth becomes greater than 90 cm by the end of July in the fen. The patterns of thawing permafrost presented here

are consistent with Deng et al. (2014), who simulated the same site using the DNDC model.

### 3.2.2 CO<sub>2</sub> exchanges

The daily Net Ecosystem Exchange (NEE) simulated in the CTRL simulation reasonably captures observed seasonal dynamics from 2003 to 2007 for all the examined peatland types (Figure 5). The simulations and observations generally showed net CO<sub>2</sub> uptake (with some episodic CO<sub>2</sub> emissions) during summer and release during winter. The observations and simulations also showed large CO<sub>2</sub> emissions in the palsa site during fall of 2004. Simulated fall CO<sub>2</sub> bursts in the three sites in other years could not be confirmed because of a lack of observations during these periods. Similar to the patterns reported in Raz-Yaseef et al. (2016), some episodic CO<sub>2</sub> emission pulses were simulated as surface ice thaws in spring, but there were no measurements to confirm those events. The correlation coefficients of the simulated and observed daily NEE ranged from 0.58 to 0.60, and most of the discrepancies between the simulations and observations were within the ranges of NEE variability measured at different subsites (automated chambers) within the same peatland type.

As described in section 2.2, simulated CO<sub>2</sub> exchanges were evaluated for 3-hourly and daily time steps when quality-controlled measurements were available ( $R^2$  values and relative root mean squared errors (RRMSEs) shown in Table 2). Simulated NEE is in reasonable agreement with the 3-hourly NEE measurements with RRMSEs ranging from 8.4 to 19.1%. Model comparisons with observations were generally poorer at daily time steps, although the calculated RRMSEs were comparable to those reported in Deng

et al. (2014). We suspect these differences resulted from uncertainty in determining an accurate observed daily NEE representative of the entire peatland type due to (1) limited daily data points (less than 14% across the study period, Table 1) due to lack of continuous quality-controlled 3-hourly measurements and (2) the large variability of daily NEE ranges measured at different subsites within the same peatland type (Figure 5). Our results thus indicate that NEE is affected by thaw stage (Bäckstrand et al., 2010; Deng et al., 2014) and fine scale spatial heterogeneity of the system. More detailed measurements with higher spatial and temporal resolutions within the same peatland type would be necessary to characterize the effects of this type of heterogeneity.

### 3.2.3 Water table depth and CH<sub>4</sub> exchanges

Simulated water table depth generally captures observed seasonal patterns measured in the bog and fen sites from 2003 to 2007 (Figure 6a, c). During summer, the predicted bog water table depth fluctuates around the ground surface (-7 to -1 cm), and the predicted water table depth is at or above the ground surface in the fen. Water table depths simulated by *ecosys* are generally higher than measured in the bog, where measured water table depths are often below the ground surface with greater seasonal variability. Simulated fen water table depths have better overall fit to observations, being higher (~5 cm) than measurements in 2003 and 2004, close to measurements in 2005 and 2006, and slightly deeper (~2 cm) than measurements in 2007. These differences in modeled and observed water table depth could be driven by the limitations of our one-dimensional column simulation which inhibits lateral water transport and hinders the variations of water table depth, which is a particular issue in simulating the dynamic

water table of the bog. A multi-dimensional simulation that includes realistic topographic effects could help improve the representation of water table dynamics, and estimates of the measurement uncertainty would help facilitate the assessment of simulation bias.

Simulated and measured daily CH<sub>4</sub> exchanges correlate reasonably well in the bog ( $r = 0.49$ ) and well in the fen ( $r = 0.65$ ) across the study period (Figure 6b, d). Both the simulations and observations have stronger CH<sub>4</sub> emissions during summer with peak emissions in late summer. Some episodic CH<sub>4</sub> emission pulses (Mastepanov et al., 2008) were simulated during shoulder seasons, and the simulated amount of post-growing season CH<sub>4</sub> emissions agrees well with those measured in 2007.

Most of the discrepancies between simulated and observed CH<sub>4</sub> emissions were within the variability of measurements across subsites within the same peatland type. The 3-hourly and daily RRMSEs ranged from 11.1 to 22.3% (Table 2) and the daily RRMSEs were comparable to results presented in Deng et al. (2014). Our results show that model evaluation of CH<sub>4</sub> emissions with finer temporal resolution observations is not necessarily superior to evaluation with coarser temporal resolution, as compared to the NEE counterpart, which could be related to weaker CH<sub>4</sub> emission variability measured across subsites within the same peatland type (Figure 6b, d).

### 3.3 Variability across the permafrost thaw gradient

Thaw rate and ALD increase along the thaw gradient (i.e., palsa to bog to fen), and landscape variations are generally greater than simulated inter-annual variability (Figure 7a). Maximum carbon uptake also increases along the thaw gradient, and variations across the landscape are comparable with simulated intra-seasonal and inter-

annual variabilities (Figure 7b). The simulated mean seasonal cumulative NEE were calculated based on the seasonality identified in Bäckstrand et al. (2010), and the results show that the magnitude of mean growing season CO<sub>2</sub> uptake is highest in the fen and lowest in the palsa (Table 3). The same rank applies to the magnitude of mean CO<sub>2</sub> emissions over the non-growing season, although differences across the thaw gradient are smaller.

CH<sub>4</sub> emission rates increase significantly along the thaw gradient, and the palsa site emissions are negligible (Figure 7c). Mean cumulative CH<sub>4</sub> emissions simulated in the fen are much higher than those in the bog, and most CH<sub>4</sub> emissions occur during the growing season (Table 3). The higher CH<sub>4</sub> emissions in the fen can be attributed to its faster seasonal thaw rate (Figure 7a) and a water table depth close to the surface (Figure 6c). Seasonal cumulative NEE and CH<sub>4</sub> emissions from observations could not be accessed due to the lack of continuous quality controlled carbon flux measurements during our study period (Table 1).

## **4. Climate sensitivity of permafrost thaw**

### **4.1 Thaw responses to climate**

For each of the four sets of simulations with different climate forcing (section 2.5), simulated mean ALD from 2003 to 2007 is always greatest in the fen and lowest in the palsa (Figure 8). This consistent trend along the thaw gradient indicates that ALDs are largely regulated by their distinct ecological and hydrological conditions, because all three sites had the same climate forcing in each set of simulations (i.e., CTRL, BIASED-COLD, BIASED-WET, and BIASED-COLD&BIASED-WET). Therefore, the palsa,

bog, and fen have different resilience against the changes in climate forcing, and this type of ecosystem resilience plays an important role in determining ALD under changes in climate conditions.

Effects of climate on simulated ALD are similar across peatland types (Figure 8). With increased precipitation (BIASED-WET vs. CTRL), simulated ALD generally becomes deeper with greater inter-annual variability because the increased snowpack depth keeps the soil warmer with lower soil ice content during winter. This effect is less prominent in the comparison between experiments BIASED-COLD and BIASED-COLD&BIASED-WET, because the cold biases in these two experiments (section 3.1) constrain ALD development. For example, summertime soil heating in some of the simulation years was not strong enough to thaw the soil ice between 20-40 cm completely in the BIASED-COLD&BIASED-WET run, resulting in shallower ALDs simulated in the palsa and fen even with the snowpack warming effect. The simulated ALD also becomes deeper with higher air temperature (CTRL vs. BIASED-COLD; BIASED-WET vs. BIASED-COLD&BIASED-WET) at all the examined peatland types. This response is more evident in the comparison between experiments BIASED-WET and BIASED-COLD&BIASED-WET, probably driven by their wet biases (section 3.1) that facilitate ALD deepening (via increased thermal conductivity and advective heat transport; Grant et al. 2017a). Similar dependencies between ALD and climate were shown in Åkerman and Johansson (2008) and Johansson et al. (2013), based on multi-year measurements and snow manipulation experiments.

Therefore, the combined cold and wet biases in the GSWP3 climate reanalysis dataset could counteract their individual effects on simulated ALD development at the



Stordalen Mire. Our results indicate a 28.6%, 0.7%, and 11.7% underestimation of ALD simulated in the palsa, bog, and fen, respectively, when applying the GSWP3 climate reanalysis data over this region without proper bias correction (BIASED-COLD&BIASED-WET vs. CTRL). Our sensitivity analysis suggests that projected warming and wetting trends (Collins et al., 2013) could significantly increase ALD in the Arctic, since increases in precipitation and air temperature can both contribute to ALD deepening.

## 4.2 Carbon budget responses to climate

Simulations with the four climate forcing datasets (section 2.5) indicate annual mean (from 2003 to 2007) CO<sub>2</sub> sinks and CH<sub>4</sub> sources, except the weak CO<sub>2</sub> emissions simulated in the fen in experiment BIASED-COLD&BIASED-WET due to reduced sedge productivity driven by increased temperature and oxygen stresses (Figure 9a,b). Our results also indicate that differences in annual CO<sub>2</sub> and CH<sub>4</sub> exchanges across the four climate forcing datasets for a single peatland type are as large as those across peatland types for a single climate forcing dataset (Figure 9a,b). These large CO<sub>2</sub> and CH<sub>4</sub> exchanges climate sensitivities demonstrate that the peatland's dynamical responses to climate have stronger effects on the carbon cycle than on ALDs (Figure 8).

With bias-corrected precipitation, increased air temperature (CTRL vs. BIASED-COLD) leads to stronger CO<sub>2</sub> uptake and greater CH<sub>4</sub> emissions at all the examined peatland types (Figure 9a,b), mainly because enhanced sedge growth facilitates carbon cycling under a warmer environment (results not shown). This air temperature sensitivity affects CO<sub>2</sub> and CH<sub>4</sub> exchanges within the same peatland type without significantly

changing ALD (Figure 8). For both experiments, CO<sub>2</sub> uptake and CH<sub>4</sub> emissions are greatest in the fen and lowest in the palsa, consistent with the measurements reported in Bäckstrand et al. (2010) for the same period. Based on the Coupled Model Intercomparison Project, phase 5 (CMIP5) ESM simulations, arctic annual mean surface air temperature is projected to increase by 8.5±2.1 °C over the 21<sup>st</sup> century (Bintanja and Andry, 2017). This projected air temperature increase is more than double the air temperature difference between site-observed and GSWP3 temperatures, which could significantly enhance CH<sub>4</sub> emissions regardless of palsa degradation into bog and fen.

On the other hand, wet biases (BIASED-WET and BIASED-COLD&BIASED-WET) increase CH<sub>4</sub> emissions in the palsa; wetter and colder conditions result in as much CH<sub>4</sub> release as the current fen, while wetter conditions alone drive palsa emissions comparable to the current bog (Figure 9b). The large precipitation sensitivity found in palsa CH<sub>4</sub> emissions could have strong effects on palsa carbon cycling because arctic precipitation is projected to increase by 50 – 60% towards the end of the 21<sup>st</sup> century (based on CMIP5 estimates; Bintanja and Andry, 2017). The comparison between experiments BIASED-WET and BIASED-COLD&BIASED-WET shows that in the palsa, increased air temperature strengthens CO<sub>2</sub> uptake and weakens CH<sub>4</sub> emissions. This shift is primarily driven in the model by increased shrub and moss productivity under the warmer environment, which facilitate CO<sub>2</sub> uptake while drying out the soil and reducing CH<sub>4</sub> emissions (results not shown). In the bog and fen sites, increased air temperature under wet bias strengthens both the simulated CO<sub>2</sub> uptake and CH<sub>4</sub> emissions (BIASED-WET vs. BIASED-COLD&BIASED-WET), due to enhanced sedge growth under the warmer environment that facilitates carbon cycling in the experiment

BIASED-WET. The low CH<sub>4</sub> emissions in bog and fen simulated in experiment  
BIASED-COLD&BIASED-WET are driven by increased temperature and oxygen  
stresses that greatly reduce heterotrophic respiration (CH<sub>4</sub> production) and sedge cover  
(aerenchyma transport).

We assessed the integrated effects of the changes in CO<sub>2</sub> and CH<sub>4</sub> exchanges  
identified in the full suite of simulations in terms of the Net Carbon Balance (NCB) and  
net emissions of greenhouse gases expressed as CO<sub>2</sub> equivalents (Net Greenhouse Gas  
Balance; NGGB). NCB was defined as the sum of the annual total CO<sub>2</sub> and CH<sub>4</sub>  
exchanges. NGGB was defined in a similar fashion as the NCB, but considers the greater  
radiative forcing potential of CH<sub>4</sub> than CO<sub>2</sub> (28 times over a 100-year horizon, Myhre et  
al., 2013) when calculating the annual total. The calculated NCB values are mostly  
negative because the stronger CO<sub>2</sub> uptake dominates the weaker CH<sub>4</sub> emissions (Figure  
9c). The results suggest that all the examined peatland types serve as net carbon sinks  
under current climate (CTRL), consistent with the estimates reported in Deng et al.  
(2014) and Lundin et al. (2016). We find a 24, 36, and 38 g C m<sup>-2</sup> y<sup>-1</sup> underestimation of  
NCB simulated in the palsa, bog, and fen sites, respectively, due to the cold and wet  
biases in the GSWP3 climate reanalysis dataset (BIASED-COLD&BIASED-WET vs.  
CTRL). NGGB is affected more strongly by CH<sub>4</sub> emissions (Figure 9d) due to its larger  
radiative forcing potential. NGGB values are positive over the bog and fen, suggesting  
that these sites have positive radiative forcing impacts despite being net carbon sinks.  
NGGB simulated in the palsa is generally negative (i.e., a net sink from the atmosphere)  
due to lower CH<sub>4</sub> emissions, except for the simulation conducted without any climate bias  
correction (correcting only air temperature increased CH<sub>4</sub> emissions but not enough to

compensate for the significantly higher CO<sub>2</sub> sink). Our results indicate that the simulated NGGB would be biased by 298, -66, and -252 g CO<sub>2</sub>-eq m<sup>-2</sup> y<sup>-1</sup> in the palsa, bog, and fen, respectively, without proper bias correction for the GSWP3 climate reanalysis dataset (BIASED-COLD&BIASED-WET vs. CTRL). Using the GSWP3 products directly thus effectively eliminates the positive radiative forcing from the expanding bog and fen, while creating a potentially dramatically inaccurate positive radiative forcing from the shrinking palsa.

#### **4.3 Climate sensitivity versus landscape heterogeneity**

Climate sensitivity and landscape heterogeneity are defined here as variability across the four climate forcing datasets for a single peatland type, and variability across three peatland types with bias-corrected climate (CTRL), respectively. We estimated carbon cycle variability associated with climate sensitivity and landscape heterogeneity to quantify the corresponding uncertainty in our annual carbon cycle assessments from 2003 to 2007. Our results indicate that differences in simulated annual mean CO<sub>2</sub> exchanges and NCB from climate sensitivity are greater than those from landscape heterogeneity (Figure 9a,c); i.e., annual CO<sub>2</sub> uptake strength is more sensitive to climate forcing uncertainty than to peatland type representation. In terms of the simulated annual mean CH<sub>4</sub> emissions and NGGB, our results indicate that variability from climate sensitivity is comparable to those from landscape heterogeneity (Figure 9b,d). Therefore, bias-corrected climate and realistic peatland characterization are both necessary to reduce the uncertainty in representing carbon cycling dynamics and their radiative forcing effects.

In addition to **their** effects on carbon cycle predictions, changes in climate conditions also affect permafrost degradation and thus induce changes in areal cover of peatland types. Malmer et al. (2005) showed that there were -0.95, 0.24, and 0.62 ha areal cover changes (-10.3%, 4.0%, and 46.3% percentage changes) from 1970 to 2000 in palsa, bog, and fen, respectively, at the Stordalen Mire. By applying the annual mean CO<sub>2</sub> and CH<sub>4</sub> exchanges simulated with bias-corrected climate from 2003 to 2007, the areal cover changes from 1970 to 2000 alone would lead to -44 kg C y<sup>-1</sup>, 76 kg C y<sup>-1</sup>, and 2076 kg CO<sub>2</sub>-eq y<sup>-1</sup> changes in annual mean CO<sub>2</sub> exchanges, CH<sub>4</sub> exchanges, and NGGB, respectively, at the Stordalen Mire. The changes in landscape-scale carbon cycle dynamics indicate that the radiative warming impact of increased CH<sub>4</sub> emissions is large enough to offset the radiative cooling impact of increased CO<sub>2</sub> uptake at the Stordalen Mire, consistent with the estimates reported in Deng et al. (2014). The areal cover changes across peatland types could persist or accelerate under the projected warming and wetting trends in the Arctic (Collins et al., 2013; Bintanja and Andry, 2017), which could stimulate CH<sub>4</sub> emissions and produce a stronger radiative warming impact.

## **5. Conclusions**

We evaluated the climate bias in a widely used atmospheric reanalysis product (GSWP3) at our northern Sweden Stordalen Mire site. We then applied a comprehensive biogeochemistry model, *ecosys*, to estimate the effects of these biases on active layer development and carbon cycling across a thaw gradient at the site. Our results show that *ecosys* reasonably represented measured hydrological, thermal, and biogeochemical cycle processes in the intact permafrost palsa, partly thawed bog, and fen. We found that the

cold and wet biases in the GSWP3 climate reanalysis dataset significantly alter model simulations, leading to biases in simulated Active Layer Depths, Net Carbon Balance, and Net Greenhouse Gas Balance by up to 28.6%, 38 g C m<sup>-2</sup> y<sup>-1</sup>, and 298 g CO<sub>2</sub>-eq m<sup>-2</sup> y<sup>-1</sup>, respectively. The Net Carbon Balance simulated with bias-corrected climate suggests that all the examined peatland types are currently net carbon sinks from the atmosphere, although the bog and fen sites can have positive radiative forcing impacts due to their higher CH<sub>4</sub> emissions.

Our results indicate that the annual means of ALD, CO<sub>2</sub> uptake, and CH<sub>4</sub> emissions generally increase along the permafrost thaw gradient at the Stordalen Mire under current climate, consistent with previous studies in this region. Our analysis suggests that palsa, bog, and fen differ strongly in their carbon cycling dynamics and have different responses to climate forcing biases. Differences in simulated CO<sub>2</sub> and CH<sub>4</sub> exchanges driven by uncertainty from climate forcing are as large as those from landscape heterogeneity across the examined permafrost thaw gradient. Model simulations demonstrate that the palsa site exhibits the strongest sensitivity to biases in air temperature and precipitation. The wet bias in GSWP3 could erroneously increase predicted CH<sub>4</sub> emissions from the palsa site to a magnitude comparable to emissions currently measured in the bog and fen sites. These results also show that increased precipitation projected for high latitude regions could strongly accelerate CH<sub>4</sub> emissions from the palsa area, even without degradation of palsa into bog and fen. Future studies should thus recognize the effects of climate forcing uncertainty on carbon cycling, in addition to tracking changes in carbon budgets associated with areal changes in permafrost degradation.

600

601 **Acknowledgements**

602 This study was funded by the Genomic Science Program of the United States Department  
603 of Energy Office of Biological and Environmental Research under the ISOGENIE  
604 project, grant DE-SC0016440, to Lawrence Berkeley Laboratory under contract DE-  
605 AC02-05CH11231, and by support from the Swedish Research Council (VR) to PMC.  
606 We thank the Abisko Scientific Research Station of the Swedish Polar Research  
607 Secretariat for providing the meteorological data.

608

## References

- Ahlström, A., Schurgers, G. and Smith, B.: The large influence of climate model bias on terrestrial carbon cycle simulations, *Environmental Research Letters*, 12(1), 014004, doi:[10.1088/1748-9326/12/1/014004](https://doi.org/10.1088/1748-9326/12/1/014004), 2017.
- Anav, A., Friedlingstein, P., Kidston, M., Bopp, L., Ciais, P., Cox, P., Jones, C., Jung, M., Myneni, R. and Zhu, Z.: Evaluating the Land and Ocean Components of the Global Carbon Cycle in the CMIP5 Earth System Models, *J. Climate*, 26(18), 6801–6843, doi:10.1175/JCLI-D-12-00417.1, 2013.
- Arneth, A., Sitch, S., Pongratz, J., Stocker, B. D., Ciais, P., Poulter, B., Bayer, A. D., Bondeau, A., Calle, L., Chini, L. P., Gasser, T., Fader, M., Friedlingstein, P., Kato, E., Li, W., Lindeskog, M., Nabel, J. E. M. S., Pugh, T. A. M., Robertson, E., Viovy, N., Yue, C. and Zaehle, S.: Historical carbon dioxide emissions caused by land-use changes are possibly larger than assumed, *Nature Geoscience*, 10(2), 79–84, doi:[10.1038/ngeo2882](https://doi.org/10.1038/ngeo2882), 2017.
- Bäckstrand, K., Crill, P. M., Mastepanov, M., Christensen, T. R. and Bastviken, D.: Non-methane volatile organic compound flux from a subarctic mire in Northern Sweden, *Tellus B*, 60(2), 226–237, doi:[10.1111/j.1600-0889.2007.00331.x](https://doi.org/10.1111/j.1600-0889.2007.00331.x), 2008a.
- Bäckstrand, K., Crill, P. M., Mastepanov, M., Christensen, T. R. and Bastviken, D.: Total hydrocarbon flux dynamics at a subarctic mire in northern Sweden, *Journal of Geophysical Research: Biogeosciences*, 113(G3), doi:[10.1029/2008JG000703](https://doi.org/10.1029/2008JG000703), 2008b.



631 Backstrand, K., Crill, P. M., ski, M. J.-K., Mastepanov, M., Christensen, T. R. and  
 632 Bastviken, D.: Annual carbon gas budget for a subarctic peatland, Northern  
 633 Sweden, 14, 2010.

634 Berrisford, P., Dee, D. P., Poli, P., Brugge, R., Fielding, K., Fuentes, M., Kållberg, P. W.,  
 635 Kobayashi, S., Uppala, S. and Simmons, A.: The ERA-Interim archive Version  
 636 2.0, 2011.

637 Bintanja, R. and Andry, O.: Towards a rain-dominated Arctic, Nature Climate Change,  
 638 7(4), 263–267, doi:[10.1038/nclimate3240](https://doi.org/10.1038/nclimate3240), 2017.

639 Callaghan, T. V., Bergholm, F., Christensen, T. R., Jonasson, C., Kokfelt, U. and  
 640 Johansson, M.: A new climate era in the sub-Arctic: Accelerating climate changes  
 641 and multiple impacts, Geophysical Research Letters, 37(14),  
 642 doi:10.1029/2009GL042064, 2010.

643 Chang, K.-Y., Paw U, K. T. and Chen, S.-H.: The importance of carbon-nitrogen  
 644 biogeochemistry on water vapor and carbon fluxes as elucidated by a multiple  
 645 canopy layer higher order closure land surface model, Agricultural and Forest  
 646 Meteorology, 259, 60–74, doi:10.1016/j.agrformet.2018.04.009, 2018.

647 Christensen, T. R., Johansson, T., Åkerman, H. J., Mastepanov, M., Malmer, N., Friborg,  
 648 T., Crill, P. and Svensson, B. H.: Thawing sub-arctic permafrost: Effects on  
 649 vegetation and methane emissions, Geophysical Research Letters, 31(4),  
 650 doi:[10.1029/2003GL018680](https://doi.org/10.1029/2003GL018680), 2004.

651 Collins, M., R. Knutti, J. Arblaster, J.-L. Dufresne, T. Fichefet, P. Friedlingstein, X. Gao,  
 652 W.J. Gutowski, T. Johns, G. Krinner, M. Shongwe, C. Tebaldi, A.J. Weaver and  
 653 M. Wehner, 2013: Long-term Climate Change: Projections, Commitments and

654 Irreversibility. Climate Change 2013: The Physical Science Basis. Contribution of  
 655 Working Group I to the Fifth Assessment Report of the Intergovernmental Panel  
 656 on Climate Change. T. F. Stocker et al., Eds., Cambridge University Press, 1029-  
 657 1136.

658 Compo, G. P., Whitaker, J. S., Sardeshmukh, P. D., Matsui, N., Allan, R. J., Yin, X.,  
 659 Gleason, B. E., Vose, R. S., Rutledge, G., Bessemoulin, P., Brönnimann, S.,  
 660 Brunet, M., Crouthamel, R. I., Grant, A. N., Groisman, P. Y., Jones, P. D., Kruk,  
 661 M. C., Kruger, A. C., Marshall, G. J., Maugeri, M., Mok, H. Y., Nordli, Ø., Ross,  
 662 T. F., Trigo, R. M., Wang, X. L., Woodruff, S. D. and Worley, S. J.: The  
 663 Twentieth Century Reanalysis Project, Quarterly Journal of the Royal  
 664 Meteorological Society, 137(654), 1–28, doi:[10.1002/qj.776](https://doi.org/10.1002/qj.776), 2011.

665 Cooper, M. D. A., Estop-Aragonés, C., Fisher, J. P., Thierry, A., Garnett, M. H.,  
 666 Charman, D. J., Murton, J. B., Phoenix, G. K., Treharne, R., Kokelj, S. V., Wolfe,  
 667 S. A., Lewkowicz, A. G., Williams, M. and Hartley, I. P.: Limited contribution of  
 668 permafrost carbon to methane release from thawing peatlands, Nature Climate  
 669 Change, 7(7), 507–511, doi:[10.1038/nclimate3328](https://doi.org/10.1038/nclimate3328), 2017.

670 Cox, P. M., Betts, R. A., Jones, C. D., Spall, S. A. and Totterdell, I. J.: Acceleration of  
 671 global warming due to carbon-cycle feedbacks in a coupled climate model, 408,  
 672 4, 2000.

673 Deng, J., Li, C., Frolking, S., Zhang, Y., Bäckstrand, K. and Crill, P.: Assessing effects of  
 674 permafrost thaw on C fluxes based on multiyear modeling across a permafrost  
 675 thaw gradient at Stordalen, Sweden, Biogeosciences, 11(17), 4753–4770,  
 676 doi:[10.5194/bg-11-4753-2014](https://doi.org/10.5194/bg-11-4753-2014), 2014.

677 Dimitrov, D. D., Bhatti, J. S. and Grant, R. F.: The transition zones (ecotone) between  
678 boreal forests and peatlands: Ecological controls on ecosystem productivity along  
679 a transition zone between upland black spruce forest and a poor forested fen in  
680 central Saskatchewan, *Ecological Modelling*, 291, 96–108,  
681 doi:10.1016/j.ecolmodel.2014.07.020, 2014.

682 Dimitrov Dimitre D., Grant Robert F., Lafleur Peter M. and Humphreys Elyn R.:  
683 Modeling the effects of hydrology on gross primary productivity and net  
684 ecosystem productivity at Mer Bleue bog, *Journal of Geophysical Research:*  
685 *Biogeosciences*, 116(G4), doi:10.1029/2010JG001586, 2011.

686 Dirmeyer, P. A.: A History and Review of the Global Soil Wetness Project (GSWP),  
687 *Journal of Hydrometeorology*, 12(5), 729–749, doi:[10.1175/JHM-D-10-05010.1](https://doi.org/10.1175/JHM-D-10-05010.1),  
688 2011.

689 Friedlingstein, P., Cox, P., Betts, R., Bopp, L., von Bloh, W., Brovkin, V., Cadule, P.,  
690 Doney, S., Eby, M., Fung, I., Bala, G., John, J., Jones, C., Joos, F., Kato, T.,  
691 Kawamiya, M., Knorr, W., Lindsay, K., Matthews, H. D., Raddatz, T., Rayner, P.,  
692 Reick, C., Roeckner, E., Schnitzler, K.-G., Schnur, R., Strassmann, K., Weaver,  
693 A. J., Yoshikawa, C. and Zeng, N.: Climate–Carbon Cycle Feedback Analysis:  
694 Results from the C<sup>4</sup> MIP Model Intercomparison, *Journal of Climate*, 19(14),  
695 3337–3353, doi:[10.1175/JCLI3800.1](https://doi.org/10.1175/JCLI3800.1), 2006.

696 Friedlingstein, P., Meinshausen, M., Arora, V. K., Jones, C. D., Anav, A., Liddicoat, S.  
697 K. and Knutti, R.: Uncertainties in CMIP5 Climate Projections due to Carbon  
698 Cycle Feedbacks, *Journal of Climate*, 27(2), 511–526, doi:[10.1175/JCLI-D-12-](https://doi.org/10.1175/JCLI-D-12-00579.1)  
699 [00579.1](https://doi.org/10.1175/JCLI-D-12-00579.1), 2014.

700 Ghimire, B., Riley, W. J., Koven, C. D., Mu, M. and Randerson, J. T.: Representing leaf  
 701 and root physiological traits in CLM improves global carbon and nitrogen cycling  
 702 predictions, *Journal of Advances in Modeling Earth Systems*, 8(2), 598–613,  
 703 doi:[10.1002/2015MS000538](https://doi.org/10.1002/2015MS000538), 2016.

704 Grant, R. F.: Modelling changes in nitrogen cycling to sustain increases in forest  
 705 productivity under elevated atmospheric CO<sub>2</sub> and contrasting site conditions,  
 706 *Biogeosciences*, 10(11), 7703–7721, doi:10.5194/bg-10-7703-2013, 2013.

707 Grant, R. F.: Nitrogen mineralization drives the response of forest productivity to soil  
 708 warming: Modelling in ecosys vs. measurements from the Harvard soil heating  
 709 experiment, *Ecological Modelling*, 288, 38–46,  
 710 doi:10.1016/j.ecolmodel.2014.05.015, 2014.

711 Grant R. F. and Flanagan L. B.: Modeling stomatal and nonstomatal effects of water  
 712 deficits on CO<sub>2</sub> fixation in a semiarid grassland, *Journal of Geophysical*  
 713 *Research: Biogeosciences*, 112(G3), doi:10.1029/2006JG000302, 2007.

714 Grant, R. F. and Roulet, N. T.: Methane efflux from boreal wetlands: Theory and testing  
 715 of the ecosystem model Ecosys with chamber and tower flux measurements,  
 716 *Global Biogeochemical Cycles*, 16(4), 2-1-2–16, doi:10.1029/2001GB001702,  
 717 2002.

718 Grant, R. F., Oechel, W. C. and Ping, C.-L.: Modelling carbon balances of coastal arctic  
 719 tundra under changing climate, *Global Change Biology*, 9(1), 16–36,  
 720 doi:10.1046/j.1365-2486.2003.00549.x, 2003.

721 Grant, R. F., Black, T. A., Humphreys, E. R. and Morgenstern, K.: Changes in net  
 722 ecosystem productivity with forest age following clearcutting of a coastal

723 Douglas-fir forest: testing a mathematical model with eddy covariance  
 724 measurements along a forest chronosequence, *Tree Physiol.*, 27(1), 115–131,  
 725 2007a.

726 Grant, R. F., Arkebauer, T. J., Dobermann, A., Hubbard, K. G., Schimelfenig, T. T.,  
 727 Suyker, A. E., Verma, S. B. and Walters, D. T.: Net Biome Productivity of  
 728 Irrigated and Rainfed Maize–Soybean Rotations: Modeling vs. Measurements,  
 729 *Agronomy Journal*, 99(6), 1404, doi:10.2134/agronj2006.0308, 2007b.

730 Grant, R. F., Barr, A. G., Black, T. A., Gaumont-Guay, D., Iwashita, H., Kidson, J.,  
 731 McCaUGHEY, H., Morgenstern, K., Murayama, S., Nesic, Z., Saigusa, N.,  
 732 Shashkov, A. and Zha, T.: Net ecosystem productivity of boreal jack pine stands  
 733 regenerating from clearcutting under current and future climates, *Global Change*  
 734 *Biology*, 13(7), 1423–1440, doi:10.1111/j.1365-2486.2007.01363.x, 2007c.

735 Grant, R. F., Margolis, H. A., Barr, A. G., Black, T. A., Dunn, A. L., Bernier, P. Y. and  
 736 Bergeron, O.: Changes in net ecosystem productivity of boreal black spruce  
 737 stands in response to changes in temperature at diurnal and seasonal time scales,  
 738 *Tree Physiology*, 29(1), 1–17, doi:10.1093/treephys/tpn004, 2009a.

739 Grant, R. F., Barr, A. G., Black, T. A., Margolis, H. A., Dunn, A. L., Metsaranta, J.,  
 740 Wang, S., McCaughey, J. H. and Bourque, C. A.: Interannual variation in net  
 741 ecosystem productivity of Canadian forests as affected by regional weather  
 742 patterns – A Fluxnet-Canada synthesis, *Agricultural and Forest Meteorology*,  
 743 149(11), 2022–2039, doi:10.1016/j.agrformet.2009.07.010, 2009b.

744 Grant, R. F., Hutrya, L. R., Oliveira, R. C., Munger, J. W., Saleska, S. R. and Wofsy, S.  
 745 C.: Modeling the carbon balance of Amazonian rain forests: resolving ecological

746 controls on net ecosystem productivity, *Ecological Monographs*, 79(3), 445–463,  
 747 doi:10.1890/08-0074.1, 2009c.

748 Grant, R. F., Barr, A. G., Black, T. A., Margolis, H. A., Mccaughey, J. H. and Trofymow,  
 749 J. A.: Net ecosystem productivity of temperate and boreal forests after  
 750 clearcutting—a Fluxnet-Canada measurement and modelling synthesis, *Tellus B:*  
 751 *Chemical and Physical Meteorology*, 62(5), 475–496, doi:10.1111/j.1600-  
 752 0889.2010.00500.x, 2010.

753 Grant, R. F., Kimball, B. A., Conley, M. M., White, J. W., Wall, G. W. and Ottman, M.  
 754 J.: Controlled Warming Effects on Wheat Growth and Yield: Field Measurements  
 755 and Modeling, *Agronomy Journal*, 103(6), 1742–1754,  
 756 doi:10.2134/agronj2011.0158, 2011a.

757 Grant, R. F., Humphreys, E. R., Lafleur, P. M. and Dimitrov, D. D.: Ecological controls  
 758 on net ecosystem productivity of a mesic arctic tundra under current and future  
 759 climates, *Journal of Geophysical Research: Biogeosciences*, 116(G1),  
 760 doi:10.1029/2010JG001555, 2011b.

761 Grant, R. F., Baldocchi, D. D. and Ma, S.: Ecological controls on net ecosystem  
 762 productivity of a seasonally dry annual grassland under current and future  
 763 climates: Modelling with ecosys, *Agricultural and Forest Meteorology*, 152, 189–  
 764 200, doi:10.1016/j.agrformet.2011.09.012, 2012a.

765 Grant, R. F., Desai, A. R. and Sulman, B. N.: Modelling contrasting responses of wetland  
 766 productivity to changes in water table depth, *Biogeosciences*, 9(11), 4215–4231,  
 767 doi:10.5194/bg-9-4215-2012, 2012b.

768 Grant R. F., Humphreys E. R. and Lafleur P. M.: Ecosystem CO<sub>2</sub> and CH<sub>4</sub> exchange in a  
 769 mixed tundra and a fen within a hydrologically diverse Arctic landscape: 1.  
 770 Modeling versus measurements, Journal of Geophysical Research:  
 771 Biogeosciences, 120(7), 1366–1387, doi:10.1002/2014JG002888, 2015.

772 Grant, R. F., Mekonnen, Z. A., Riley, W. J., Wainwright, H. M., Graham, D. and Torn,  
 773 M. S.: Mathematical Modelling of Arctic Polygonal Tundra with Ecosys: 1.  
 774 Microtopography Determines How Active Layer Depths Respond to Changes in  
 775 Temperature and Precipitation, Journal of Geophysical Research: Biogeosciences,  
 776 122(12), 3161–3173, doi:[10.1002/2017JG004035](https://doi.org/10.1002/2017JG004035), 2017a.

777 Grant, R. F., Mekonnen, Z. A., Riley, W. J., Arora, B. and Torn, M. S.: Mathematical  
 778 Modelling of Arctic Polygonal Tundra with *Ecosys*: 2. Microtopography  
 779 Determines How CO<sub>2</sub> and CH<sub>4</sub> Exchange Responds to Changes in Temperature  
 780 and Precipitation: GHG Exchange in Arctic Polygonal Tundra, Journal of  
 781 Geophysical Research: Biogeosciences, 122(12), 3174–3187,  
 782 doi:[10.1002/2017JG004037](https://doi.org/10.1002/2017JG004037), 2017b.

783 Guo, D., Wang, H. and Wang, A.: Sensitivity of Historical Simulation of the Permafrost  
 784 to Different Atmospheric Forcing Data Sets from 1979 to 2009, Journal of  
 785 Geophysical Research: Atmospheres, 122(22), 12,269–12,284,  
 786 doi:[10.1002/2017JD027477](https://doi.org/10.1002/2017JD027477), 2017.

787 Harris, I., Jones, P. D., Osborn, T. J. and Lister, D. H.: Updated high-resolution grids of  
 788 monthly climatic observations – the CRU TS3.10 Dataset, International Journal of  
 789 Climatology, 34(3), 623–642, doi:10.1002/joc.3711, n.d.

790 Hodgkins, S. B., Tfaily, M. M., McCalley, C. K., Logan, T. A., Crill, P. M., Saleska, S.  
 791 R., Rich, V. I. and Chanton, J. P.: Changes in peat chemistry associated with  
 792 permafrost thaw increase greenhouse gas production, *Proceedings of the National*  
 793 *Academy of Sciences*, 111(16), 5819–5824, doi:[10.1073/pnas.1314641111](https://doi.org/10.1073/pnas.1314641111), 2014.  
 794 van den Hurk, B., Kim, H., Krinner, G., Seneviratne, S. I., Derksen, C., Oki, T., Douville,  
 795 H., Colin, J., Ducharne, A., Cheruy, F., Viovy, N., Puma, M. J., Wada, Y., Li, W.,  
 796 Jia, B., Alessandri, A., Lawrence, D. M., Weedon, G. P., Ellis, R., Hagemann, S.,  
 797 Mao, J., Flanner, M. G., Zampieri, M., Matera, S., Law, R. M. and Sheffield, J.:  
 798 LS3MIP (v1.0) contribution to CMIP6: the Land Surface, Snow and Soil moisture  
 799 Model Intercomparison Project – aims, setup and expected outcome,  
 800 *Geoscientific Model Development*, 9(8), 2809–2832, doi:10.5194/gmd-9-2809-  
 801 2016, 2016.  
 802 Hugelius, G., Strauss, J., Zubrzycki, S., Harden, J. W., Schuur, E. A. G., Ping, C.-L.,  
 803 Schirrmeister, L., Grosse, G., Michaelson, G. J., Koven, C. D.,  
 804 O&apos;Donnell, J. A., Elberling, B., Mishra, U., Camill, P., Yu, Z.,  
 805 Palmtag, J. and Kuhry, P.: Estimated stocks of circumpolar permafrost carbon  
 806 with quantified uncertainty ranges and identified data gaps, *Biogeosciences*,  
 807 11(23), 6573–6593, doi:10.5194/bg-11-6573-2014, 2014.  
 808 IPCC, 2014: Climate Change 2014: Synthesis Report. Contribution of Working Groups I,  
 809 II and III to the Fifth Assessment Report of the Intergovernmental Panel on  
 810 Climate Change [Core Writing Team, R.K. Pachauri and L.A. Meyer (eds.)].  
 811 IPCC, Geneva, Switzerland, 151 pp.



812 Johansson, M., Callaghan, T. V., Bosiö, J., Åkerman, H. J., Jackowicz-Korczynski, M.  
813 and Christensen, T. R.: Rapid responses of permafrost and vegetation to  
814 experimentally increased snow cover in sub-arctic Sweden, *Environmental*  
815 *Research Letters*, 8(3), 035025, doi:[10.1088/1748-9326/8/3/035025](https://doi.org/10.1088/1748-9326/8/3/035025), 2013.

816 Johansson, T., Malmer, N., Crill, P. M., Friberg, T., Åkerman, J. H., Mastepanov, M. and  
817 Christensen, T. R.: Decadal vegetation changes in a northern peatland, greenhouse  
818 gas fluxes and net radiative forcing, *Global Change Biology*, 12(12), 2352–2369,  
819 doi:[10.1111/j.1365-2486.2006.01267.x](https://doi.org/10.1111/j.1365-2486.2006.01267.x), 2006.

820 Jones, M. C., Harden, J., O'Donnell, J., Manies, K., Jorgenson, T., Treat, C. and Ewing,  
821 S.: Rapid carbon loss and slow recovery following permafrost thaw in boreal  
822 peatlands, *Glob. Chang. Biol.*, 23(3), 1109–1127, doi:[10.1111/gcb.13403](https://doi.org/10.1111/gcb.13403), 2017.

823 Kalnay, E., Kanamitsu, M., Kistler, R., Collins, W., Deaven, D., Gandin, L., Iredell, M.,  
824 Saha, S., White, G., Woollen, J., Zhu, Y., Chelliah, M., Ebisuzaki, W., Higgins,  
825 W., Janowiak, J., Mo, K. C., Ropelewski, C., Wang, J., Leetmaa, A., Reynolds,  
826 R., Jenne, R. and Joseph, D.: The NCEP/NCAR 40-Year Reanalysis Project, *Bull.*  
827 *Amer. Meteor. Soc.*, 77(3), 437–472, doi:[10.1175/1520-](https://doi.org/10.1175/1520-0477(1996)077<0437:TNYP>2.0.CO;2)  
828 [0477\(1996\)077<0437:TNYP>2.0.CO;2](https://doi.org/10.1175/1520-0477(1996)077<0437:TNYP>2.0.CO;2), 1996.

829 Kanamitsu, M., Ebisuzaki, W., Woollen, J., Yang, S.-K., Hnilo, J. J., Fiorino, M. and  
830 Potter, G. L.: NCEP–DOE AMIP-II Reanalysis (R-2), *Bull. Amer. Meteor. Soc.*,  
831 83(11), 1631–1644, doi:[10.1175/BAMS-83-11-1631](https://doi.org/10.1175/BAMS-83-11-1631), 2002.

832 Kokfelt, U., Reuss, N., Struyf, E., Sonesson, M., Rundgren, M., Skog, G., Rosen, P., and  
833 Hammarlund, D.: Wetland development, permafrost history and nutrient cycling

834 inferred from late Holocene peat and lake sediment records in subarctic Sweden,  
835 J. Paleolimn., 44, 327–342, doi:10.1007/s10933-010-9406- 8, 2010.

836 Lundin, E. J., Klaminder, J., Giesler, R., Persson, A., Olefeldt, D., Heliasz, M.,  
837 Christensen, T. R. and Karlsson, J.: Is the subarctic landscape still a carbon sink?  
838 Evidence from a detailed catchment balance, Geophysical Research Letters,  
839 43(5), 1988–1995, doi:[10.1002/2015GL066970](https://doi.org/10.1002/2015GL066970), 2016.

840 Malmer, N., Johansson, T., Olsrud, M. and Christensen, T. R.: Vegetation, climatic  
841 changes and net carbon sequestration in a North-Scandinavian subarctic mire over  
842 30 years, Global Change Biology, 11(11), 1895–1909, doi:[10.1111/j.1365-](https://doi.org/10.1111/j.1365-2486.2005.01042.x)  
843 [2486.2005.01042.x](https://doi.org/10.1111/j.1365-2486.2005.01042.x), 2005.

844 Mastepanov, M., Sigsgaard, C., Dlugokencky, E. J., Houweling, S., Ström, L., Tamstorf,  
845 M. P. and Christensen, T. R.: Large tundra methane burst during onset of  
846 freezing, Nature, 456(7222), 628–630, doi:[10.1038/nature07464](https://doi.org/10.1038/nature07464), 2008.

847 McCalley, C. K., Woodcroft, B. J., Hodgkins, S. B., Wehr, R. A., Kim, E.-H., Mondav,  
848 R., Crill, P. M., Chanton, J. P., Rich, V. I., Tyson, G. W. and Saleska, S. R.:  
849 Methane dynamics regulated by microbial community response to permafrost  
850 thaw, Nature, 514(7523), 478–481, doi:[10.1038/nature13798](https://doi.org/10.1038/nature13798), 2014.

851 Mezbahuddin, M., Grant, R. F. and Hirano, T.: Modelling effects of seasonal variation in  
852 water table depth on net ecosystem CO<sub>2</sub> exchange of a tropical peatland,  
853 Biogeosciences, 11(3), 577–599, doi:[10.5194/bg-11-577-2014](https://doi.org/10.5194/bg-11-577-2014), 2014.

854 Mondav, R., McCalley, C. K., Hodgkins, S. B., Frolking, S., Saleska, S. R., Rich, V. I.,  
855 Chanton, J. P. and Crill, P. M.: Microbial network, phylogenetic diversity and  
856 community membership in the active layer across a permafrost thaw gradient,

857 Environmental Microbiology, 19(8), 3201–3218, doi:[10.1111/1462-2920.13809](https://doi.org/10.1111/1462-2920.13809),  
858 2017.

859 Mondav, R., Woodcroft, B. J., Kim, E.-H., McCalley, C. K., Hodgkins, S. B., Crill, P.  
860 M., Chanton, J., Hurst, G. B., VerBerkmoes, N. C., Saleska, S. R., Hugenholtz, P.,  
861 Rich, V. I. and Tyson, G. W.: Discovery of a novel methanogen prevalent in  
862 thawing permafrost, Nature Communications, 5, 3212, doi:[10.1038/ncomms4212](https://doi.org/10.1038/ncomms4212),  
863 2014.

864 Myhre, G., D. Shindell, F.-M. Bréon, W. Collins, J. Fuglestedt, J. Huang, D. Koch, J.-F.  
865 Lamarque, D. Lee, B. Mendoza, T. Nakajima, A. Robock, G. Stephens, T.  
866 Takemura and H. Zhang, 2013: Anthropogenic and Natural Radiative Forcing. In:  
867 Climate Change 2013: The Physical Science Basis. Contribution of Working  
868 Group I to the Fifth Assessment Report of the Intergovernmental Panel on  
869 Climate Change [Stocker, T.F., D. Qin, G.-K. Plattner, M. Tignor, S.K. Allen, J.  
870 Boschung, A. Nauels, Y. Xia, V. Bex and P.M. Midgley (eds.)]. Cambridge  
871 University Press, Cambridge, United Kingdom and New York, NY, USA, pp.  
872 659–740, doi:10.1017/CBO9781107415324.018.

873 O'Donnell, J. A., Jorgenson, M. T., Harden, J. W., McGuire, A. D., Kanevskiy, M. Z. and  
874 Wickland, K. P.: The Effects of Permafrost Thaw on Soil Hydrologic, Thermal,  
875 and Carbon Dynamics in an Alaskan Peatland, Ecosystems, 15(2), 213–229,  
876 doi:[10.1007/s10021-011-9504-0](https://doi.org/10.1007/s10021-011-9504-0), 2012.

877 Olefeldt, D. and Roulet, N. T.: Effects of permafrost and hydrology on the composition  
878 and transport of dissolved organic carbon in a subarctic peatland complex, Journal

879 of Geophysical Research: Biogeosciences, 117(G1), doi:[10.1029/2011JG001819](https://doi.org/10.1029/2011JG001819),  
880 2012.

881 Piao, S., Liu, Z., Wang, T., Peng, S., Ciais, P., Huang, M., Ahlstrom, A., Burkhardt, J. F.,  
882 Chevallier, F., Janssens, I. A., Jeong, S.-J., Lin, X., Mao, J., Miller, J.,  
883 Mohammat, A., Myneni, R. B., Peñuelas, J., Shi, X., Stohl, A., Yao, Y., Zhu, Z.  
884 and Tans, P. P.: Weakening temperature control on the interannual variations of  
885 spring carbon uptake across northern lands, *Nature Climate Change*, 7(5), 359–  
886 363, doi:[10.1038/nclimate3277](https://doi.org/10.1038/nclimate3277), 2017.

887 Raz-Yaseef, N., Torn, M. S., Wu, Y., Billesbach, D. P., Liljedahl, A. K., Kneafsey, T. J.,  
888 Romanovsky, V. E., Cook, D. R. and Wullschleger, S. D.: Large CO<sub>2</sub> and CH<sub>4</sub>  
889 emissions from polygonal tundra during spring thaw in northern Alaska,  
890 *Geophysical Research Letters*, 44(1), 504–513, doi:[10.1002/2016GL071220](https://doi.org/10.1002/2016GL071220),  
891 2017.

892 Rydén, B. E., Fors, L. and Kostov, L.: Physical Properties of the Tundra Soil-Water  
893 System at Stordalen, Abisko, *Ecological Bulletins*, (30), 27–54, 1980.

894 Schuur, E. a. G., McGuire, A. D., Schädel, C., Grosse, G., Harden, J. W., Hayes, D. J.,  
895 Hugelius, G., Koven, C. D., Kuhry, P., Lawrence, D. M., Natali, S. M., Olefeldt,  
896 D., Romanovsky, V. E., Schaefer, K., Turetsky, M. R., Treat, C. C. and Vonk, J.  
897 E.: Climate change and the permafrost carbon feedback, *Nature*, 520(7546), 171–  
898 179, doi:[10.1038/nature14338](https://doi.org/10.1038/nature14338), 2015.

899 Sonesson, M. (1972) Cryptogams. In: International biological programme—Swedish  
900 tundra biome project. Technical report No. 9, April 1972. Swedish Natural  
901 Science Research Council Ecological Research Committee.

902 Tokida, T., Miyazaki, T., Mizoguchi, M., Nagata, O., Takakai, F., Kagemoto, A. and  
 903 Hatano, R.: Falling atmospheric pressure as a trigger for methane ebullition from  
 904 peatland, *Global Biogeochemical Cycles*, 21(2), doi:10.1029/2006GB002790,  
 905 2007.

906 Viovy, N.: CRUNCEP Version 7 - Atmospheric Forcing Data for the Community Land  
 907 Model, Research Data Archive at the National Center for Atmospheric Research,  
 908 Computational and Information Systems Laboratory, Boulder CO.

909 Wickland, K. P., Striegl, R. G., Neff, J. C. and Sachs, T.: Effects of permafrost melting  
 910 on CO<sub>2</sub> and CH<sub>4</sub> exchange of a poorly drained black spruce lowland, *Journal of*  
 911 *Geophysical Research: Biogeosciences*, 111(G2), doi:[10.1029/2005JG000099](https://doi.org/10.1029/2005JG000099),  
 912 2006.

913 Woodcroft, B. J., Singleton, C. M., Boyd, J. A., Evans, P. N., Emerson, J. B., Zayed, A.  
 914 A. F., Hoelzle, R. D., Lamberton, T. O., McCalley, C. K., Hodgkins, S. B.,  
 915 Wilson, R. M., Purvine, S. O., Nicora, C. D., Li, C., Froking, S., Chanton, J. P.,  
 916 Crill, P. M., Saleska, S. R., Rich, V. I. and Tyson, G. W.: Genome-centric view of  
 917 carbon processing in thawing permafrost, *Nature*, doi:[10.1038/s41586-018-0338-](https://doi.org/10.1038/s41586-018-0338-1)  
 918 [1](https://doi.org/10.1038/s41586-018-0338-1), 2018.

919 Wu, Z., Ahlström, A., Smith, B., Ardö, J., Eklundh, L., Fensholt, R. and Lehsten, V.:  
 920 Climate data induced uncertainty in model-based estimations of terrestrial  
 921 primary productivity, *Environmental Research Letters*, 12(6), 064013,  
 922 doi:10.1088/1748-9326/aa6fd8, 2017.

923 Yoshimura, K. and Kanamitsu, M.: Dynamical Global Downscaling of Global  
 924 Reanalysis, Monthly Weather Review, 136(8), 2983–2998,  
 925 doi:[10.1175/2008MWR2281.1](https://doi.org/10.1175/2008MWR2281.1), 2008.  
 926 Zaehle, S., Friend, A. D., Friedlingstein, P., Dentener, F., Peylin, P. and Schulz, M.:  
 927 Carbon and nitrogen cycle dynamics in the O-CN land surface model: 2. Role of  
 928 the nitrogen cycle in the historical terrestrial carbon balance, Global  
 929 Biogeochemical Cycles, 24(1), doi:[10.1029/2009GB003522](https://doi.org/10.1029/2009GB003522), 2010.  
 930 Zimov, S. A., Davydov, S. P., Zimova, G. M., Davydova, A. I., Schuur, E. a. G., Dutta,  
 931 K. and Chapin, F. S.: Permafrost carbon: Stock and decomposability of a globally  
 932 significant carbon pool, Geophysical Research Letters, 33(20),  
 933 doi:[10.1029/2006GL027484](https://doi.org/10.1029/2006GL027484), 2006.  
 934

935 Table 1. Temporal coverage of quality-controlled CO<sub>2</sub> and CH<sub>4</sub> exchanges measured by  
 936 automated chambers at the three peatland types in the Stordalen Mire during the years  
 937 2002 to 2007.

Sites	Number of data points	CO <sub>2</sub>		Number of data points	CH <sub>4</sub>	
		3 Hourly coverage (%)	Daily coverage (%)		3 Hourly coverage (%)	Daily coverage (%)
Palsa	12752	65.8	12.4	N/A	N/A	N/A
Bog	12821	68.5	12.7	6660	96.2	25.0
Fen	8989	63.8	13.7	4923	90.5	33.7

938

939 Table 2. Evaluation of the 3 hourly and daily CO<sub>2</sub> and CH<sub>4</sub> exchanges simulated at the  
 940 palsa, bog, and fen sites. RRMSEs are relative root mean squared errors.

Sites	C component	3-Hourly		Daily	
		R <sup>2</sup>	RRMSEs (%)	R <sup>2</sup>	RRMSEs (%)
Palsa	CO <sub>2</sub>	0.48	13.4	0.36	18.3
Bog	CO <sub>2</sub>	0.63	19.1	0.44	35.8
	CH <sub>4</sub>	0.31	16.3	0.47	22.3
Fen	CO <sub>2</sub>	0.64	8.4	0.43	25.5
	CH <sub>4</sub>	0.44	11.1	0.54	16.9

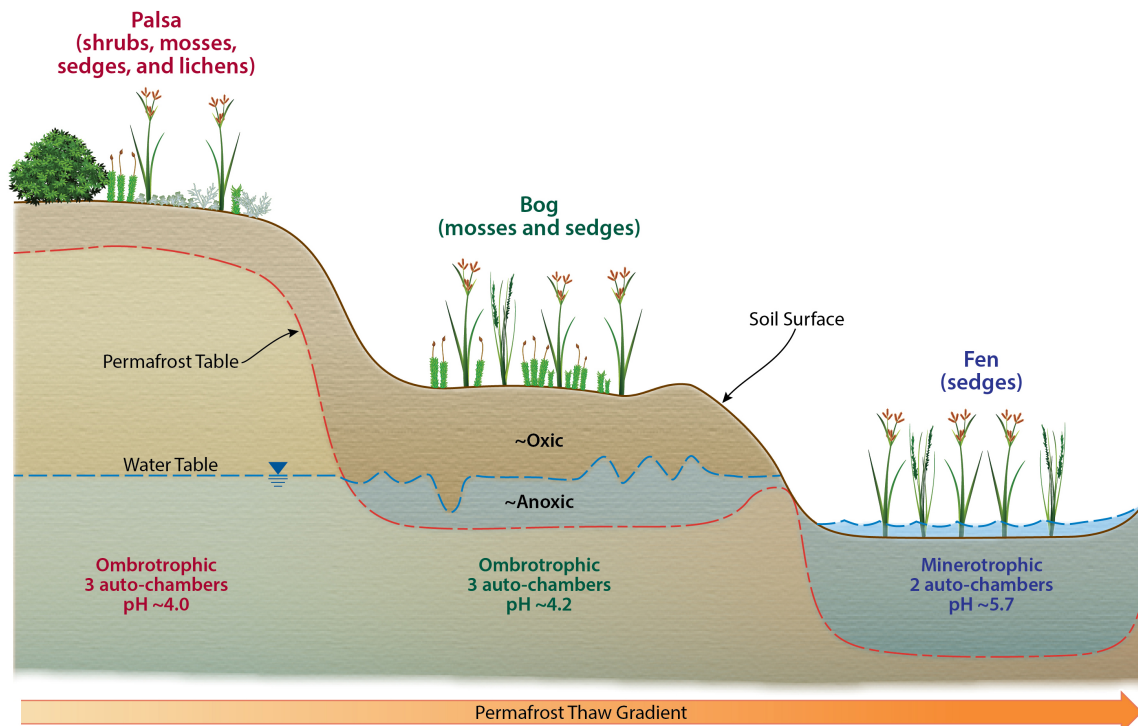
941

942



Table 3. Means and standard deviations of cumulative CO<sub>2</sub> and CH<sub>4</sub> exchanges simulated in the palsa, bog, and fen during the period 2003 to 2007. All exchanges are in units of g C m<sup>-2</sup>.

Sites	C flux component	Growing season; Days 119–288		Non-growing season; Days 1–118/289–365	
		Mean	Standard deviation	Mean	Standard deviation
Palsa	CO <sub>2</sub>	-72.70	19.10	38.89	4.09
	CH <sub>4</sub>	0.04	0.02	0.01	0.002
Bog	CO <sub>2</sub>	-79.59	21.46	42.89	2.16
	CH <sub>4</sub>	3.52	0.45	0.42	0.11
Fen	CO <sub>2</sub>	-88.65	7.26	44.41	6.13
	CH <sub>4</sub>	10.86	3.95	0.78	0.18



EESA19-008

Figure 1. Schematic diagram of the sampling sites at Stordalen Mire.

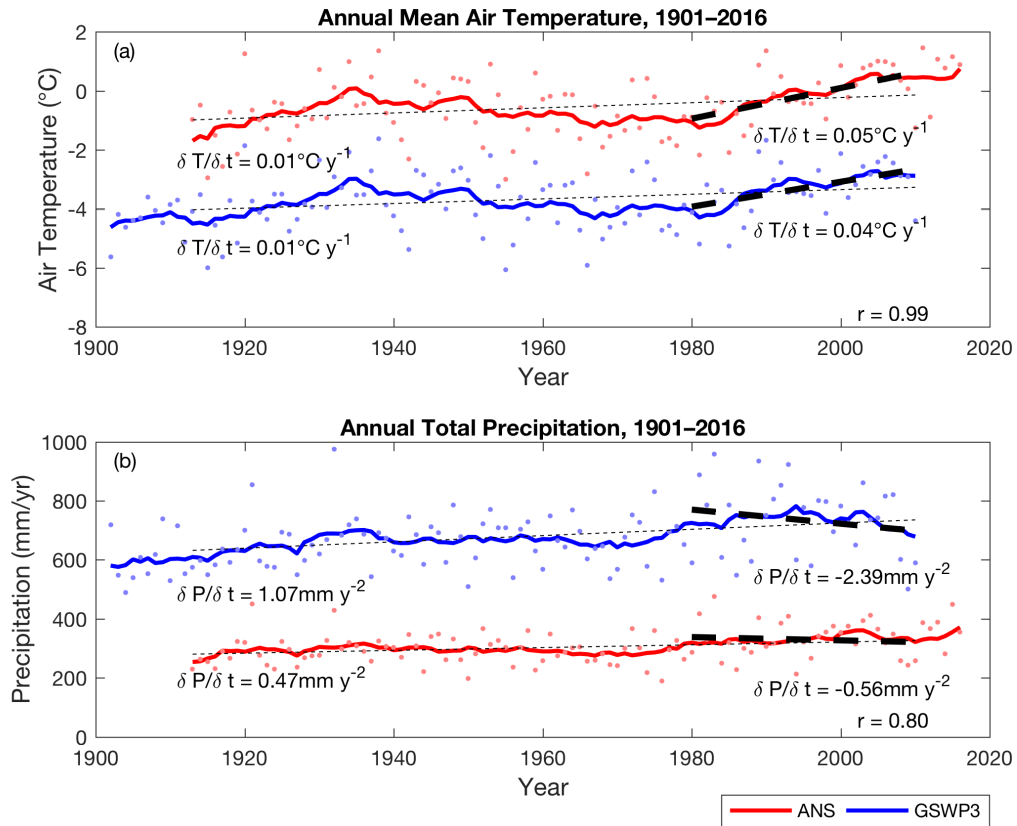


Figure 2. Time series of air temperature (a) and precipitation (b) measured at ANS (red; years 1913–2016) and extracted from GSWP3 (blue; years 1901–2010). Dots are the annual means and solid lines are the decadal moving averages of the corresponding annual means. Thin and thick dashed lines are the trends for years 1913–2010, and years 1980–2010, respectively. The inset  $r$  values are the correlation coefficients calculated between the two time series.

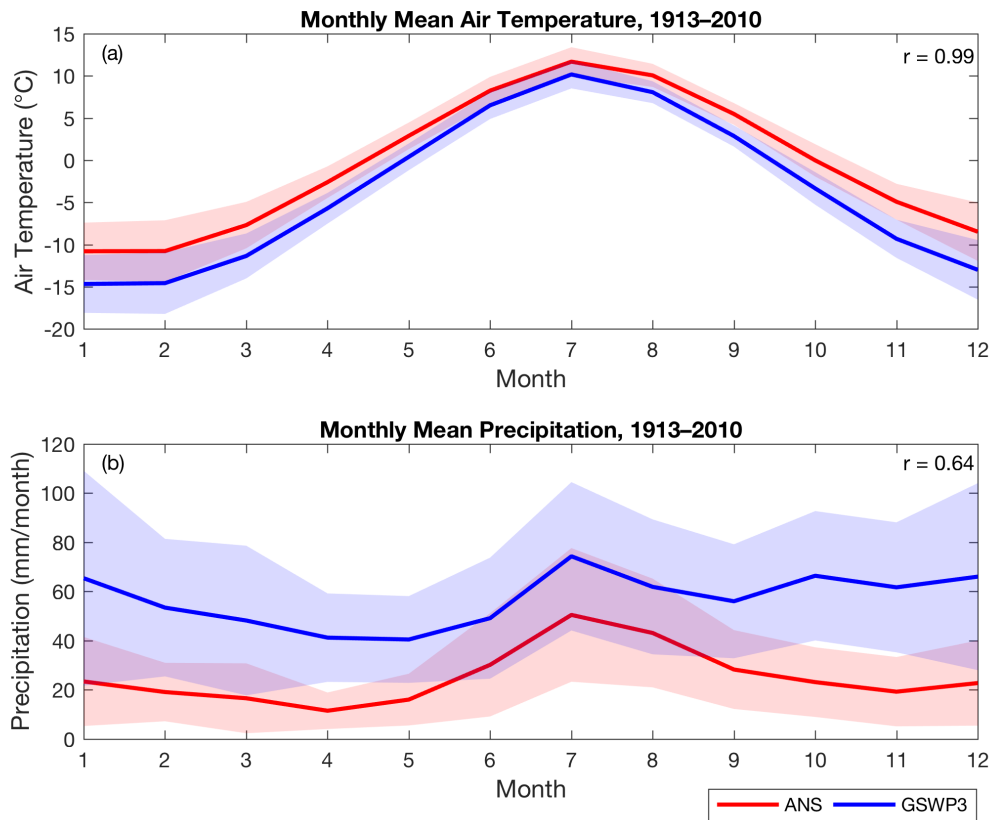


Figure 3. Monthly mean air temperature (a) and precipitation (b) measured at ANS (red) and extracted from GSWP3 (blue). The shaded area is the inter-annual variability for the corresponding dataset, represented by the standard deviations calculated at each month. The inset  $r$  values are the correlation coefficients calculated between the two time series.

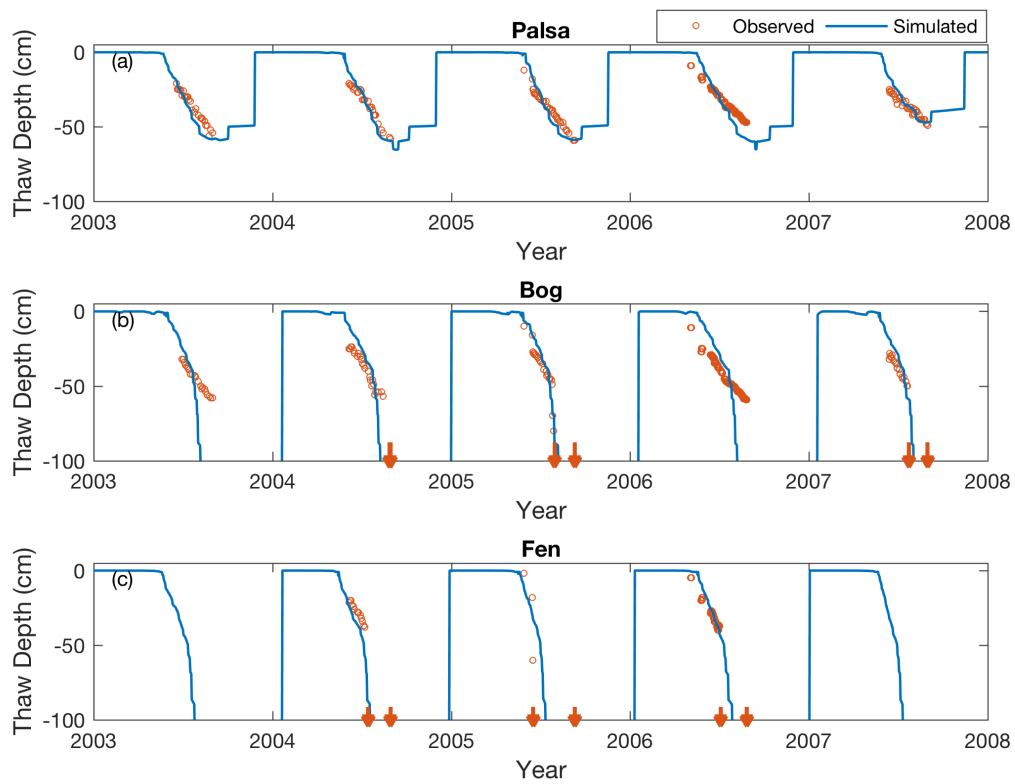


Figure 4. Simulated (solid lines) and measured (open circles) seasonal dynamics of thaw depth at the palsa (a), bog (b), and fen (c) sites from 2003 to 2007. Downward arrows indicate the time when measured thaw depth deepens below 90 cm for a measurement year.

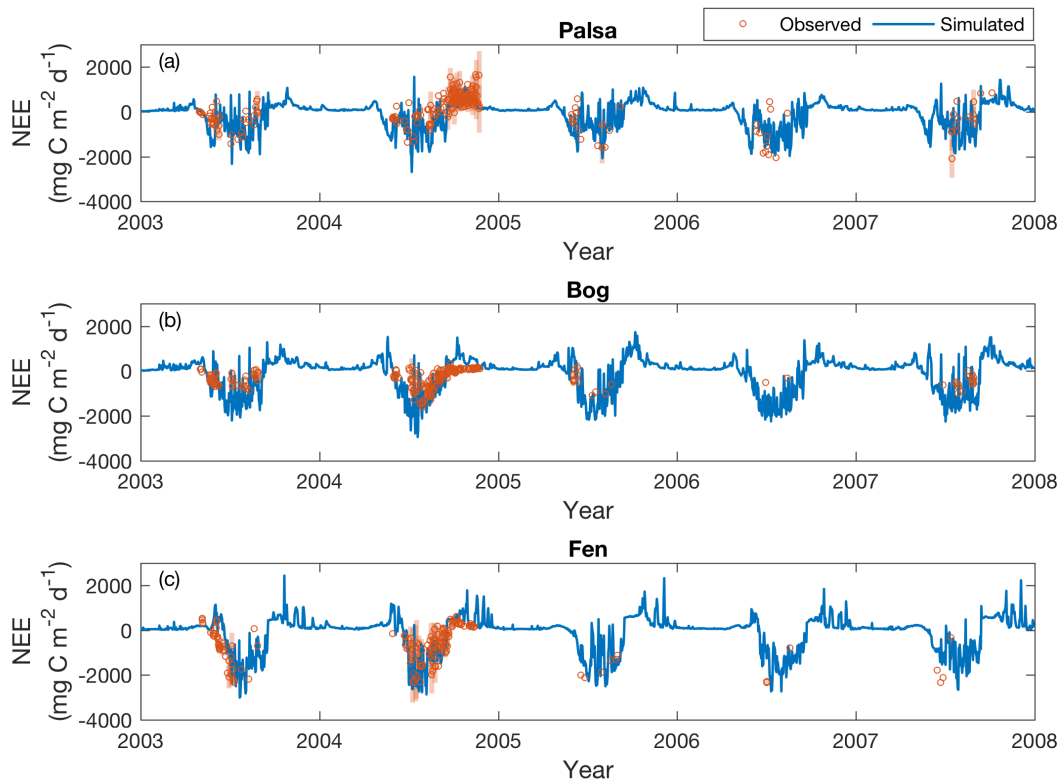
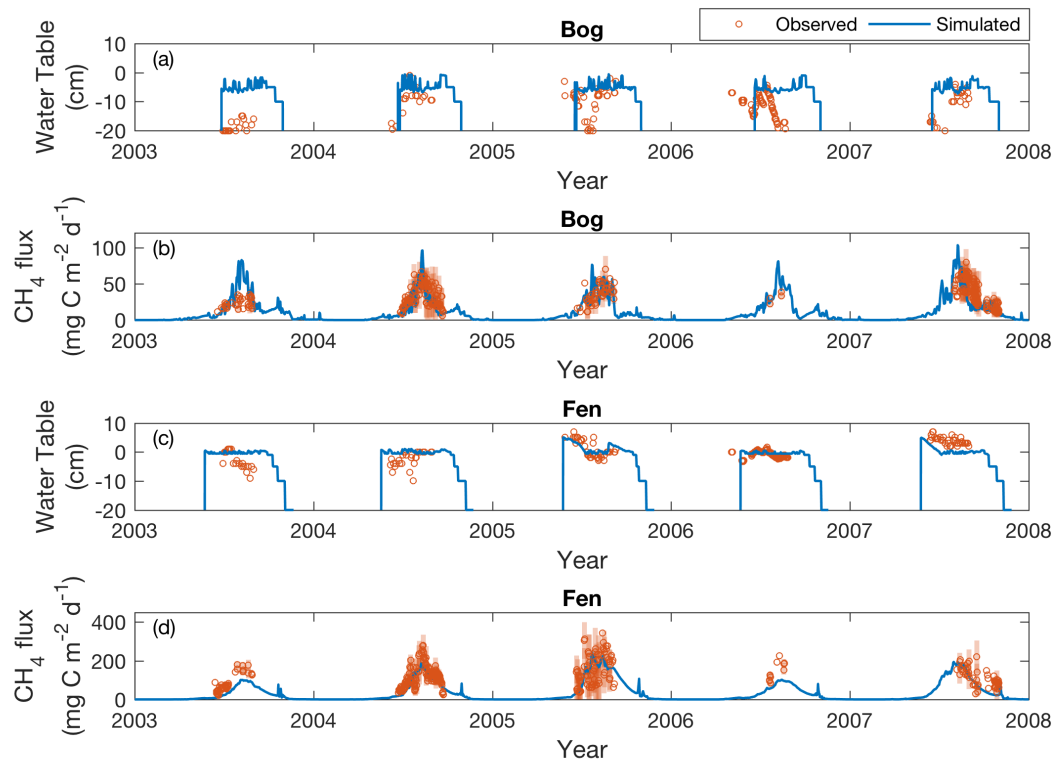


Figure 5. Simulated (solid lines) and measured (open circles) daily CO<sub>2</sub> exchanges (NEE) at the palsa (a), bog (b), and fen (c) sites, from 2003 to 2007. Shaded bars are the standard deviations of daily NEE measured across subsites under each peatland type. Positive and negative values indicate effluxes from and influxes to the site, respectively.



977

978 Figure 6. Simulated (solid lines) and measured (open circles) water table depth and daily  
 979  $\text{CH}_4$  emissions at the bog and fen from 2003 to 2007. Shaded bars are the standard  
 980 deviations of the daily  $\text{CH}_4$  emissions measured across the subsites under each peatland  
 981 type.

982

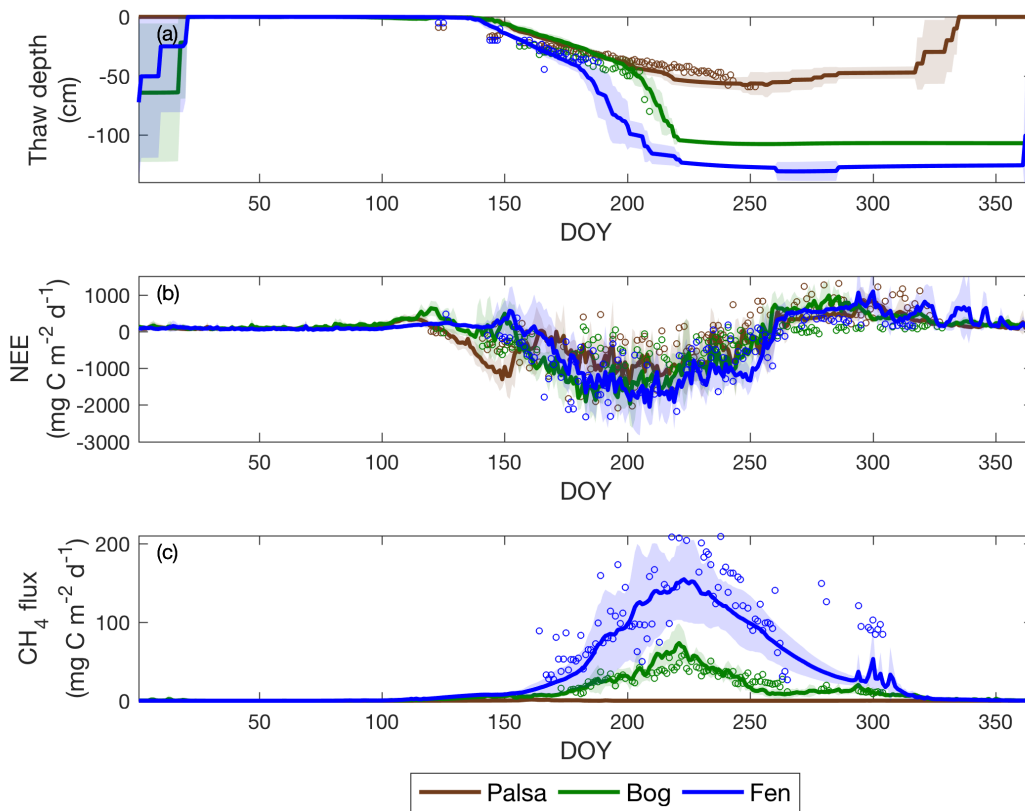


Figure 7. Daily thaw depth (a), daily NEE (b), and daily CH<sub>4</sub> (c) exchanges for the three sites from 2003 to 2007. Solid lines and open circles are the simulated and measured inter-annual means for each day of year, respectively. The shaded area is the simulated inter-annual variability for the corresponding dataset, represented by the standard deviations calculated at each day of year. Positive and negative carbon flux values indicate effluxes from and influxes to the site, respectively.



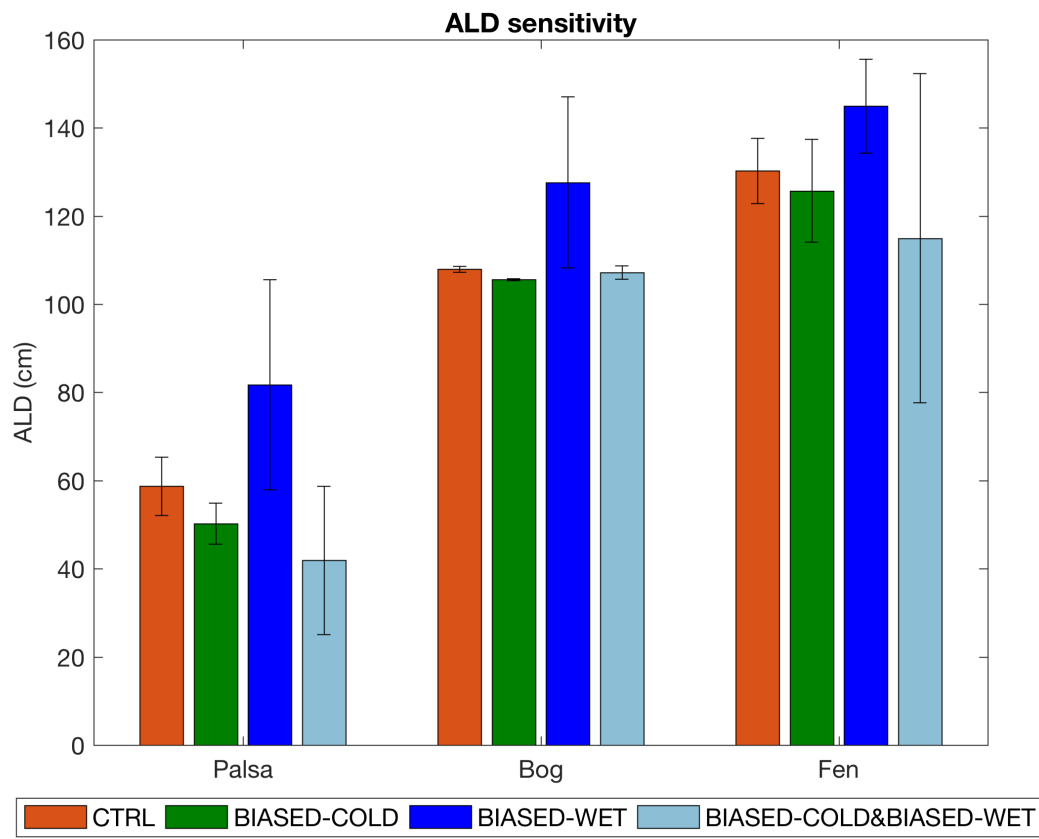


Figure 8. Simulated ALD at the palsa, bog, and fen for four sets of climate forcing (Section 2.5). Bars and error bars are means and standard deviations calculated from 2003 to 2007, respectively.

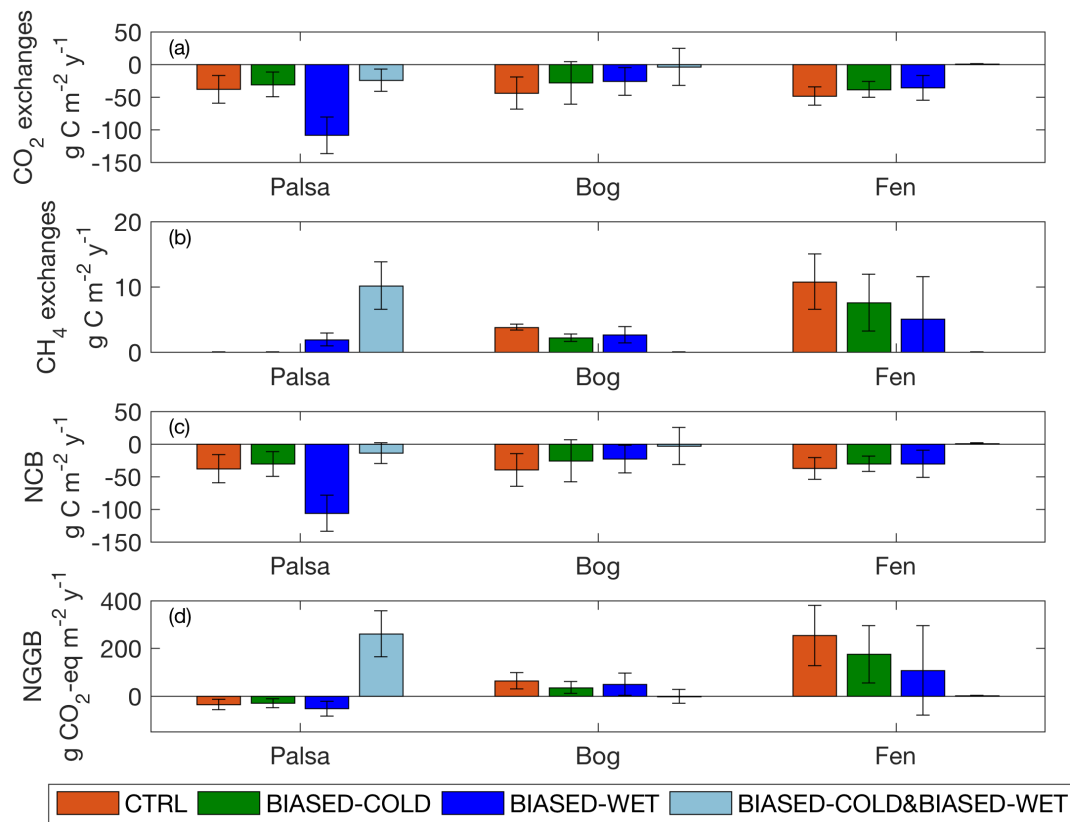


Figure 9. Annual CO<sub>2</sub> exchanges (a), CH<sub>4</sub> exchanges (b), Net Carbon Balance (c), and Net Greenhouse Gas Balance (d) simulated at the palsa, bog, and fen, under each set of simulations. Bars and error bars are the means and standard deviations calculated from 2003 to 2007, respectively. Positive and negative values indicate effluxes from and influxes to the site, respectively.